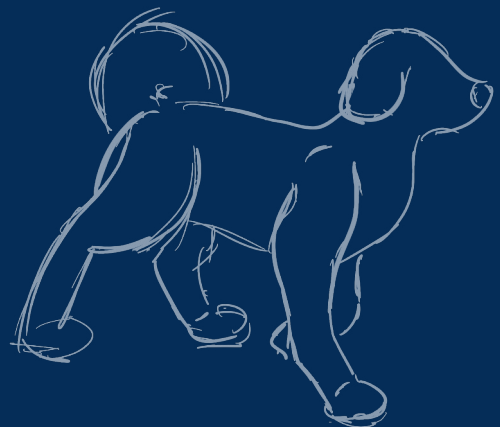
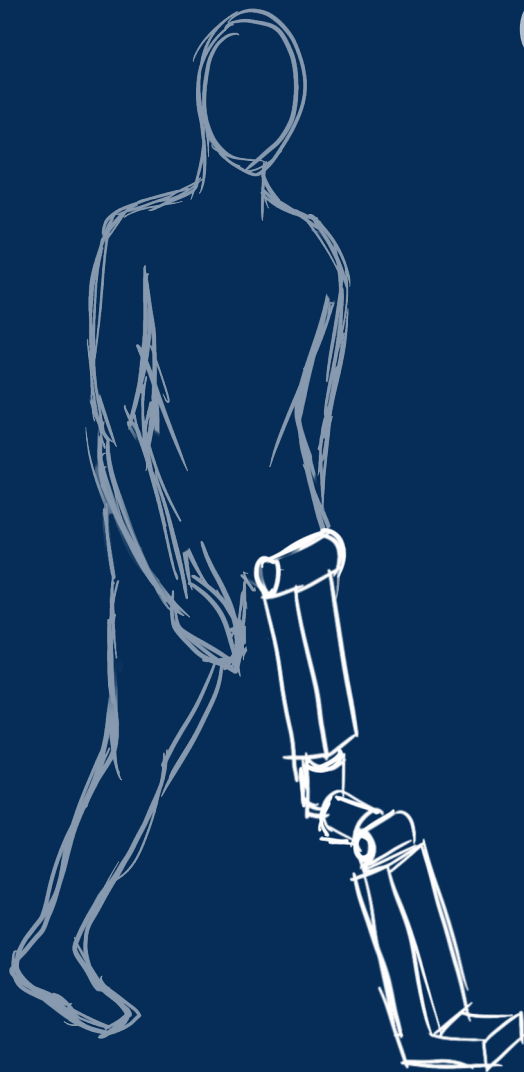


Towards an algorithm to optimise gait pattern for patients with above knee prosthesis with the use of inertial sensors

Christine Amelie Palm



Towards an algorithm to optimise gait pattern for patients with above knee prosthesis with the use of inertial sensors

by

Christine Amelie Palm

to obtain the degree of

MASTER OF SCIENCE

at the Delft University of Technology,

to be defended confidentially on the 28th of February, 2020 at 09:00.

Student number:	4746449	
Project duration:	May, 2019 – February, 2020	
Supervisors and thesis committee:	Prof. Dr.-Ing. Heike Vallery, Herman Boiten, Dr.ir. Manon Kok, Dr.ir. Gerwin Smit,	TU Delft, supervisor Move Engineering (external) TU Delft TU Delft

This thesis is confidential and cannot be made public until February, 2022.

An electronic version of this thesis is available at <http://repository.tudelft.nl/>.

Preface

My time in the Biorobotics lab at the TU Delft was more than I could ever have hoped for. I did not only find a desk where I could work, I also found the best colleagues. From Vrijmibos over a summer party to having Feuerzangenbowle, it definitely never got boring. I want to acknowledge several people in particular. Thank you Saher, Patricia and Andy for helping me when I was stuck and for picking me up when I was down. You really showed me how we can help each other grow. Thank you Daniel for rescuing me when I threw tea over my laptop even though you did not even know me at the time. And a big shout out to the rest, including but not restricted to Nathan, Aneesh, Bram, Joris, Roemer and Charlotte. All of you made every day better with coffee talks, table football, choosing plants, finding Christmas trees and drones, having a dad jokes app and the night out dancing.

I want to thank Heike for creating this amazing environment, where every single person can find their place and for taking care of our health with the weekly fruit baskets. I also want to thank her for enabling us to create tiny jungles in our offices. Heike further was an amazing mentor. Having met her in my first week in Delft over dinner, I did not even know that she was going to be one of my Professors. I definitely did not expect to be graduating under her supervision. Her way of helping you figure out the problems you bring to her is something very unique. She also taught me how important it is to phrase your ideas as precise as possible so you have a chance to communicate them to others. I learned so much from all our meetings. Thank you!

That life is a combination of circumstances has been shown to me again by Herman being my external and daily supervisor. He used to be my boss during a pre-Master internship at Ottobock in 2017. Herman is the person that really spawned my passion for prosthetics. He showed me that the tiniest improvements can change someone's life for the better. Thank you for having me in mind when you thought about a project with Heike and letting me be the interface between your ideas and the academic approach. I really appreciate that you never got tired of sparring with me when we disagreed, so we could always end up with something that we were both happy with.

I was lucky to have three supervisors from the university. Manon, being from a different department, really helped me with her knowledge about inertial sensors and how to tackle the data processing. Thank you for trusting me to be the first to work with your new IMUs. I am so grateful, that you always made time for me in your schedule, especially for reading my drafts again and again. Your comments really helped me write a better thesis. And I want to thank Gerwin for being on my supervision team even though he already had so much on his plate. His attendance in the big meetings really made a difference. Thank you, Gerwin, for always making sure to keep us on track when we wandered off into too much detail. I want to thank all my supervisors, Heike, Herman, Manon and Gerwin, to make me see that my work was so much more than the things I did not achieve.

I am very grateful to all the people that read different stages of my thesis. Thank you Lena, Esther, Carlijn, Sanne and Cathy. I especially want to thank Prajish for finding a huge mistake that everyone else overlooked and John, who proofread my work even though I haven't even met him to this day. And a big thank you to my friends for never getting tired of hearing about my ups and downs. Special thanks go out to my honeybadgers, who sustained me when I could not do it myself. Thank you for supporting me with food, plants, hugs, motivation and advice. Thank you, Vera, for always being there for me, even while being on travels in Vietnam. Thank you, Anna and Emilio for helping me make my front page so beautiful and personal. And thank you Fabian, for making me laugh when I wanted to cry.

Finally, a big thank you goes out to my family. I could not have finished this research without your support. Thank you, for picking up the pieces when I shattered them everywhere and for rehabilitating me when I momentarily forgot how to be human. Thank you, for not pressuring me to finish but to push me to create something that I am proud of. And thank you, for sharing my excitement even though half the time you had no clue what I was talking about.

Christine Amelie Palm
4746449
Delft University of Technology
Date

Table of Contents

I	Introduction	1
I-A	Motivation and research objective	1
I-B	Background and goal	2
II	Forward kinematic mapping	3
II-A	Overview	3
II-B	Angles and frames	3
II-C	Position vectors	4
II-D	Absolute enclosed angle	4
III	Inverse kinematic mapping	5
III-A	Estimated value of adjustment angle settings	5
III-B	Calculation of adjustment setting for optimal swing	5
IV	Adjustment proposition	5
V	Experimental protocol and data acquisition	6
VI	Data processing	6
VII	Sensitivity analysis of kinematic mapping	7
VIII	Results	8
VIII-A	Evaluation of mapping	8
VIII-B	Adjustment proposition	8
VIII-C	Sensitivity	8
IX	Discussion	9
IX-A	Kinematic mapping	9
IX-B	Adjustment proposition	10
IX-C	Sensitivity analysis	11
IX-D	General	11
X	Conclusion	12
	References	13
	Appendix A: Reference data	14
	Appendix B: Angles, frames and rotational matrices for forward mapping	14
	Appendix C: Alignment measurements	15
	Appendix D: Walking direction estimation	15
	Appendix E: Sensor-body orientation	16
	Appendix F: Swing phase	16
	Appendix G: Sensitivity Analysis: Hip movement	16
	Appendix H: Sensitivity Analysis: Sensor-body orientation	17
	Appendix I: Results	19
	Appendix J: Information Sheet and Consent Form	24

List of Figures

1	Frontal, sagittal and transverse plane with respect to the human body	2
2	Whip and rotation, seen in frontal plane during flexion of left knee. Illustration based on [1].	2
3	Illustration of steps taken towards an algorithm for the optimisation of the prosthetic alignment	3
4	Illustration of the kinematic mapping model: frames, angles and positions assigned to the rigid bodies and joints	3
5	Illustration of whip and rotation of the shank	4
6	Illustration of sine function components for the calculation of sigma in the frontal plane . .	4
7	Standing/sitting calibration for the sensor-body calibration, further explained in appendix C.	6
8	Frames \mathcal{W} , \mathcal{G} , \mathcal{B} and \mathcal{S} with respect to each other, with cross section through prosthetic shank while standing upright; seen in transverse plane	7
9	Estimated alignment angles δ_{est} and ϵ_{est} in prosthetic knee	8
10	Desired alignment angles δ_{opt} and ϵ_{opt} for optimal swing	9
11	Adjustment propositions δ_{prop} and ϵ_{prop} for the knee adapter alignment angles δ and ϵ	10
12	Results of the sensitivity analysis of the sensor-body orientation on the estimation of the alignment angles δ and ϵ	11
13	Illustration of kinematic mapping model with inclusion of possible orientation influence of knee adapter on socket	14
14	CPO adjusting the VR/VL-A by turning the screw on the right side of the adapter. Further, to be seen, the plate and indicator above the knee joint to trace the changes in the I/O-RA alignment.	15
15	Sensitivity analysis on hip movement input - resulting disturbed $\tilde{\delta}$	17
16	Sensitivity analysis on hip movement input - resulting disturbed $\tilde{\epsilon}$	17

List of Tables

I	Names, affiliations, description and axes notation of frames	4
II	Definition, function and allocation of angles	14
III	Sensitivity analysis on hip movement Bias on $\alpha(t)$, $\beta(t)$ and $\gamma(t)$ input angles of hip movement	17
IV	Bias on sensor-body orientation Rotations around x , y , and z axis of body frame \mathcal{B}	18
V	19
VI	Results for first participant, part I	20
VII	Results for first participant, part II	21
VIII	Results for first participant, part III	22
IX	Results for second participant	23
X	27
XI	28
XII	28
XIII	29

Notations

Abbreviations

CPO	Certified Prosthetist/Orthotist
FKM	forward kinematic model
FoWD	frame of walking direction
IMU	inertial measurement unit
I/O-RA	inwards/outwards rotational adjustment
PCA	principal component analysis
PoWD	plane of walking direction
VR/VL-A	varus/valgus adjustment

Math

r	scalar (e.g., radius)
\mathbf{r}	vector (e.g. position vector)
\mathbf{R}	matrix (e.g. rotation matrix)
\mathbf{c}	cos
\mathbf{s}	sin
\sin^{-1}	arc sin

Kinematics and dynamics

\mathcal{A}	frame of reference
x, y, z	orthogonal unit vectors describing a frame
A	a point in Cartesian space
${}^{\mathcal{A}}r_{\mathcal{A}/B}$	position vector of point B with respect to A, components expressed in frame \mathcal{A}
\mathbf{A}	defined position vector, components in walking direction fixed frame \mathcal{W}
${}^{\mathcal{A}}\mathbf{R}_{\mathcal{B}}$	rotation matrix that transforms a vector in frame \mathcal{B} to frame \mathcal{A}
α	angular input, constant
$\alpha(t)$	angular input, over time

General

r	position
l	length
g	gravity vector, magnitude of gravitational acceleration
t	time
T	period of time
N	number of points of measurement

Denotations

α_{FKM}	resulting angle from forward kinematic model
α_{est}	resulting estimated angle
α_{opt}	resulting optimised angle
α_{prop}	resulting proposed angle
$\hat{\alpha}$	disturbance due to sensitivity analysis on the sensor-body orientation
$\tilde{\alpha}$	disturbance due to sensitivity analysis on the hip movement input

Towards an algorithm to optimise gait pattern for patients with above knee prosthesis with the use of inertial sensors

Christine Amelie Palm¹

Supervision: Heike Vallery¹, Manon Kok², Gerwin Smit³, Herman Boiten⁴

Abstract—Misalignment in prosthetic legs can lead to bad posture, back pain and stump problems. A big influence therein is the alignment in the frontal and transverse plane of a prosthetic knee. This work aims to create an auxiliary tool for the prosthetist to align the prosthesis in an optimal way for the patient, with the use of inertial sensors. The goal is to estimate the current alignment in the frontal and transverse plane of the individual's knee and therewith identify the changes that should be made to achieve an optimal swing of the shank.

A forward kinematic model of the swing phase of a prosthetic knee is combined with an inverse kinematic model to estimate the adjustment setting of the individual's knee. This is done with the data from two inertial sensors on thigh and shank of the prosthetic leg of the patient. Furthermore, the desired alignment that creates an optimal swing phase is estimated. With the comparison of the estimated and the desired alignment, an adjustment proposition is calculated. In addition, a sensitivity analysis on the sensor-body orientation is conducted.

The results for the current alignment setting show a rough accumulation around the expected linear trend. Deviations and outliers are explained with mistakes during the measurement and errors in the data processing. Also, the calculation of the optimal alignment angles and proposed changes show promising results. The results for the sensitivity analysis on the sensor-body orientation show a linear trend. However, the slope is much smaller than the expected 1. This means that disturbances in the sensor-body orientation have a smaller influence on the results of the estimated alignment angles than assumed. The influence on the adjustment angle in the transverse plane is even smaller than on the one in the frontal plane. These results lead to the conclusion that there are additional factors with an impact on the calculations.

The basis towards a working algorithm is laid out. Future work on eliminating sources of error in the data processing is suggested. Among other things, a robust approach to define the walking direction has to be established. Further, an additional measurement with a motion capture system is recommended to create a better foundation for further analysis.

I. INTRODUCTION

A. Motivation and research objective

Femoral amputees have to compensate for less muscle force and knee joint complexity as well as a non-equal distribution of body weight by implementing new control strategies during walking [2], [3]. They have to overcome a difference in temporal and kinetic parameters between the prosthetic and the sound side, which leads to a decrease in symmetry and therefore a decrease in stability [4], [5]. Furthermore, resulting mechanical overload of the joints leads to a higher chance of osteoarthritis [6]. These and more factors have an impact on the overall health and posture of an amputee. The effects of incorrect alignment especially have an impact on very active amputees. The question arises, if individuals that are very active in their youth and young adulthood will have to suffer from severe consequences once they get older [5]. Therefore, until there are affordable prosthetic systems to compensate for the effects, significant efforts should be made to prevent the issue of incorrect alignment. The prosthesis should be aligned in the optimal way to ensure a smooth gait with minimal side effects for the patient; alignment thereby meaning position and orientation of stump, socket, knee joint and foot to each other [7], [3].

The correct alignment can even out pressure distribution between socket and stump which leads to less stump pain and tissue breakdown. It further gives more stability and minimizes compensation behaviour as well as gait deviations [4], [3], [7], [8]. A common prosthetic knee is connected to the socket with an adapter that provides alignment options in all three planes: sagittal, frontal and transverse. An illustration of the planes is shown in Figure 1. Until now, most research focuses on the alignment in the sagittal plane, because it influences the knee stability during standing and walking [1].

The first step of the alignment of a prosthesis is the bench alignment, done prior to the alignment on the patient. The socket is put in the right orientation, and the knee is rotated in a way to create a stable prosthetic alignment. The next step, the static alignment, is performed on the patient wearing the prosthetic, while standing upright. The static alignment should only require small changes if the bench alignment was carried out properly [9]. These steps are taught in detail to Certified Prosthetist/Orthotists (CPO) during apprenticeship and a lot of information as well as tutorial movies are available at no charge. In addition, supporting alignment tools are

¹C.A. Palm and H. Vallery are with Mechanical, Maritime and Materials Engineering (3mE), *BME/Biorobotics Lab*, TU Delft, 2628 CD Delft, Netherlands (email: c.a.palm@student.tudelft.nl, h.vallery@tudelft.nl).

²M. Kok is with Mechanical, Maritime and Materials Engineering (3mE), *Delft Center for Systems and Control*, TU Delft, 2628 CD Delft, Netherlands (email: m.kok-1@tudelft.nl).

³G. Smit is with Mechanical, Maritime and Materials Engineering (3mE), *BME/BITE*, TU Delft, 2628 CD Delft, Netherlands (email: g.smit@tudelft.nl).

⁴H. Boiten is with Move Engineering, 6715LE Ede, Netherlands (email: boiten@move-engineering.nl).

available, like PROS.A. Assembly or the L.A.S.A.R. Assembly for the bench alignment and L.A.S.A.R Posture for the static alignment [9], [10].

The static alignment is followed by the dynamic alignment, in which the CPO evaluates the patient's walk. This includes focusing on the alignment of the frontal and transverse plane. The comparatively small movements in those two planes are hard to see by the eye, which is why this final alignment demands the CPO's skill and experience to see gait deviations and react accordingly [6]. This procedure is usually conducted in iterations until little gait deviations remain. The patient's comments on feeling and comfort are also included as an indicator [3], [8], [1]. However, amputees often lack a feeling for "what is right" and will accept different alignments that are proposed to them [11], [7].

Learning a skill, like conducting the dynamical alignment of a knee prosthesis for an inexperienced CPO, builds on understanding the task and practising it in combination with helpful feedback. As changes in the frontal and transverse plane are hard to be observed with the naked eye, computer assistance could aid the teaching immensely. In the process of a total knee arthroplasty, for example, computer assistance helped the students to better understand the fundamental anatomical reference points and axis [12]. Providing accurate feedback could further support practising, which can also be used as supervision after the learning process is completed. Approaches have been made for computer assistance in the way of visualising socket moments and ground reaction forces. However, until today, such aiding devices are expensive and time-consuming [6]. According to an experienced CPO, the difficulty of teaching paired with a lack of experience of many CPOs is the reason why many people walk with an alignment that is not optimal for them. Results of misalignment can be bad posture, back pain, stump problems and even a rise in oxygen levels [7], [13], [14], [8].

Therefore, the objective of this thesis is to work towards an algorithm that can estimate the current (mis)alignment of a prosthesis with focus on the frontal and transverse plane. Thereby, we aim to predict changes that can be made to create a better alignment and a smoother gait pattern for the patient. To keep it low-cost, portable and easy to use, this

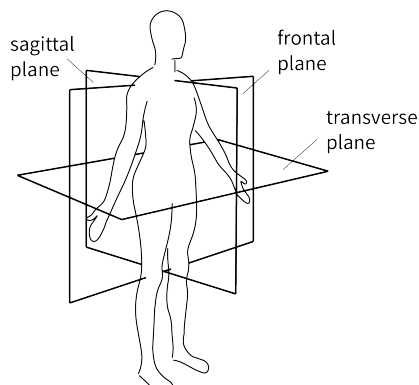


Fig. 1: Frontal, sagittal and transverse plane with respect to the human body

approach makes use of inertial measurement units (IMU) on the amputees during the alignment procedure.

B. Background and goal

Non-optimal alignment in the frontal and transverse plane of a prosthetic knee leads to changes in the walking pattern. The two most obvious indicators are whip and rotation of the shank. Both affect the movement during the swing phase of the gait. A whip is defined by a mediolateral movement of the foot and shank accompanying the natural lateral movement of the knee during swing. The natural lateral movement is induced by the femur and should be small. The whip can be seen when the shank lashes out with respect to the femur, while the upper leg swings straight through. It is illustrated in Figure 2.

The figure also illustrates the second indicator. The rotation of the shank occurs when the swing movement deviates from the straight line parallel to the walking direction. This can be seen by the toe-cap rotating out of the sagittal plane during swing [1].

Both, whip and rotation of the shank can be traced back to an incorrect alignment in the frontal and transverse plane. This means the alignment includes an incorrect amount of in-/outwards rotation and/or varus/valgus are not set in an optimal way. Achieving complete symmetry between the sound and the prosthetic side while walking is not possible for amputees, even with the perfect alignment [2]. With an incorrect alignment, coming close to symmetry is mostly achieved with compensatory mechanisms [15]. This makes symmetry an unreliable metric. Thus, instead of aiming for a symmetrical mimicking of the sound leg, the aim of this research is to achieve a straight swing of the prosthetic shank, parallel to the sagittal plane. With this approach, compensational behaviour that can lead to great discomfort can be held at a minimum [15]. Because both indicators of interest, whip and rotation of the shank, occur during swing phase, this study will be restricted to this phase of the gait cycle.

This research concentrates on predicting changes in the frontal and transverse plane alignment to get a smooth and comfortable swing phase movement parallel to the plane of

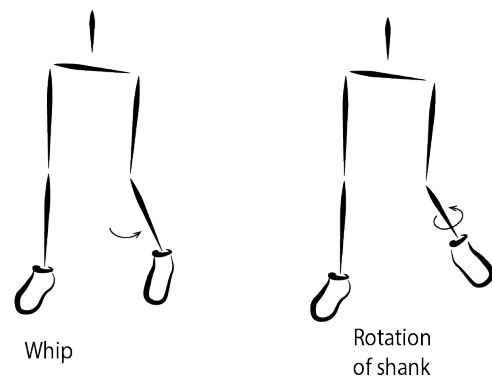


Fig. 2: Whip and rotation, seen in frontal plane during flexion of left knee. Illustration based on [1].

Frame	Affiliation	Description	Ax. Notation
\mathcal{W}	Fixed in space	Walking direction-fixed	X
\mathcal{H}_1	Hip joint	y^I aligned with Y	x^I
\mathcal{H}_2	Hip joint	x^{II} aligned with x^I	x^{II}
\mathcal{T}	Hip joint	Thigh-fixed, z^{III} aligned with z^{II}	x^{III}
\mathcal{K}_1	Knee joint	y^{IV} aligned with y^{III}	x^{IV}
\mathcal{K}_2	Knee joint	x^V aligned with x^{IV}	x^V
\mathcal{B}	Knee joint	Shank-fixed, z^{VI} aligned with z^V	x^{VI}
\mathcal{G}	Global	Magn.N-fixed, y^G aligned with Z	x^G
\mathcal{S}	Sensor	Sensor-fixed	x^S

TABLE I: Names, affiliations, description and axes notation of frames

up, the X axis points into the walking direction and Z points sideways in a right-hand frame. The frames are visualised in Figure 4 and Table I assigns all frames their names, affiliations, descriptions and axes notations. Figure and table also include frame \mathcal{G} and frame \mathcal{S} , which are part of the inertial sensor calculations and will be further explained in section VI.

In theory, there is an additional frame between the socket of the prosthesis and the prosthetic knee. It represents the position of the adapter. However, because this cannot be influenced in the work on hand, all three constitutive angles for this frame are assumed to be zero. Further, it is assumed that the adapter position is done well enough to not influence the gait of the participant. This frame is further explained in appendix B, where also a table with the allocation of angles and their respective frames can be found.

To represent all the data with respect to the FoWD \mathcal{W} , rotational matrices are defined. This represents Step 1a, as illustrated in Figure 3. First, the rotation matrix from thigh-fixed frame \mathcal{T} to the FoWD \mathcal{W} is formed as ${}^{\mathcal{W}}\mathbf{R}_{\mathcal{T}}(t)$; then, the rotation matrix from shank-fixed frame \mathcal{B} to the thigh-fixed frame ${}^{\mathcal{T}}\mathbf{R}_{\mathcal{B}}(t)$; which leads to the rotation matrix from shank-fixed frame \mathcal{B} to FoWD \mathcal{W} as ${}^{\mathcal{W}}\mathbf{R}_{\mathcal{B}}(t)$. Each rotation matrix from one frame to the next is defined as a rotation around a single axis, following the example of [17]. The rotational matrix calculations are found in more detail in Appendix B.

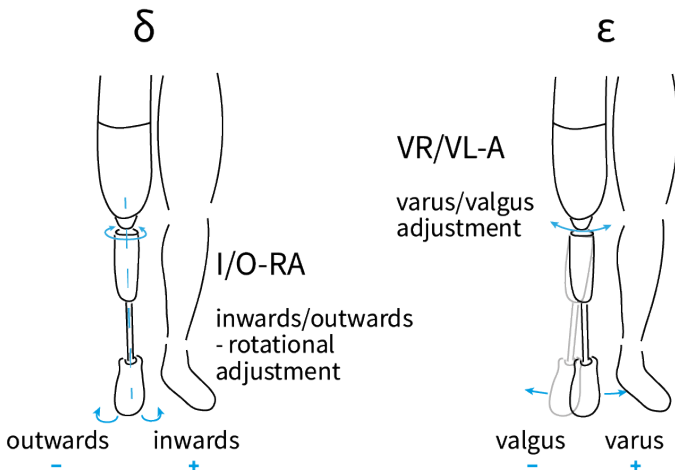


Fig. 5: Illustration of whip and rotation of the shank

C. Position vectors

With the results from Step 1a, Step 1b follows with the definition of the position vectors, as illustrated in Figure 3. To get the total angular deviation of the shank from the PoWD, the translational components of the movement have to be included. To calculate the translations, the positions of the bodies had to be defined. Point S represents the position of the shank at its end, at a length of l_S from the thigh, represented with point T . The point at the end of the foot is noted as point F at a length of l_F from point S . The vectors of point S with respect to T and point F with respect to S are given as

$${}^{\mathcal{B}}\mathbf{r}_{T/S} = \begin{bmatrix} 0 & -l_L & 0 \end{bmatrix}^T \quad \text{and} \quad (1)$$

$${}^{\mathcal{B}}\mathbf{r}_{S/F} = \begin{bmatrix} l_F & 0 & 0 \end{bmatrix}^T, \quad (2)$$

both with the components expressed in frame \mathcal{B} .

The position vectors, with their components in frame \mathcal{W} , are calculated as

$${}^{\mathcal{W}}\mathbf{r}_{T/S}(t) = {}^{\mathcal{W}}\mathbf{R}_{\mathcal{B}}(t) \cdot {}^{\mathcal{B}}\mathbf{r}_{T/S} = \mathbf{S}(t), \quad (3)$$

$${}^{\mathcal{W}}\mathbf{r}_{S/F}(t) = {}^{\mathcal{W}}\mathbf{R}_{\mathcal{B}}(t) \cdot {}^{\mathcal{B}}\mathbf{r}_{S/F} = \mathbf{F}(t), \quad (4)$$

where the vector from point S with respect to T is now named vector $\mathbf{S}(t)$ and from point F with respect to point S is now named vector $\mathbf{F}(t)$. Both vectors move over time.

D. Absolute enclosed angle

Having identified the rotational matrices (Step 1a) and the positions of the translational deviations (Step 1b), the projected angles of these deviations from the PoWD in the frontal plane are calculated (Step 1c). Figure 6 shows an exemplary calculation of $\sigma(t)$ over time. It shows the shank, as point S , with respect to the thigh, as point T , in the frontal plane. The shank and the cross section of the PoWD enclose the absolute deviation angle $\sigma(t)$, which defines the deviation from the PoWD as a rotation around the X axis of the FoWD \mathcal{W} .

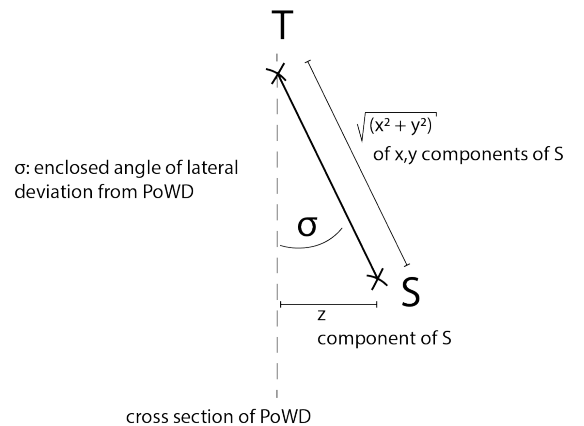


Fig. 6: Illustration of sine function components for the calculation of sigma in the frontal plane

Deviation $\sigma_{\text{FKM}}(t)$ is calculated with the trigonometric sinus function as

$${}^{\mathcal{W}}\sigma_{\text{FKM}}(\alpha(t), \beta(t), \gamma(t), \eta(t), \delta, \epsilon) = \sin^{-1} \frac{S_z(t)}{\sqrt{S_x(t)^2 + S_y(t)^2}}, \quad (5)$$

with the y component of position vector $\mathbf{S}(t)$ as the opposite leg and the length of the shank as the other hypotenuse.

The absolute enclosed angle from the PoWD in the transverse plane defines the rotation around the Z axis of frame \mathcal{W} . It is calculated as $\tau_{\text{FKM}}(t)$ with the trigonometric sinus function of the components of position vector $\mathbf{F}(t)$ as

$${}^{\mathcal{W}}\tau_{\text{FKM}}(\alpha(t), \beta(t), \gamma(t), \eta(t), \delta, \epsilon) = \sin^{-1} \frac{F_z(t)}{\sqrt{F_x(t)^2 + F_y(t)^2}}. \quad (6)$$

Both angles are referenced in frame \mathcal{W} . The subscript in both formulas (5) and (6) implies that ${}^{\mathcal{W}}\sigma_{\text{FKM}}(t)$ and ${}^{\mathcal{W}}\tau_{\text{FKM}}(t)$ are values, calculated with the forward kinematic model (FKM). Deviation over time in the frontal plane, $\sigma(t)$, represents the whip and $\tau(t)$, deviation over time in the transverse plane, represents the rotation of the shank during the swing. As the calculation of vector $\mathbf{S}(t)$ and $\mathbf{F}(t)$ in equations (3) and (4) include the rotation matrix ${}^{\mathcal{W}}\mathbf{R}_{\mathcal{B}}$, both $\sigma_{\text{FKM}}(t)$ and $\tau_{\text{FKM}}(t)$ are functions of $\alpha(t)$, $\beta(t)$, $\gamma(t)$, and $\eta(t)$ over time and a constant δ and ϵ . Further details about the rotational matrices and angles can be found in Appendix B.

III. INVERSE KINEMATIC MAPPING

A. Estimated value of adjustment angle settings

To estimate the real prosthetic alignment, the forward kinematic mapping is combined with the sensor measurements to obtain an inverse kinematic mapping. This represents Step 2 of the calculations towards the desired algorithm, illustrated in Figure 3. The inverse mapping will give us an estimation (Step 2a) for the alignment settings in the adapter above the prosthetic knee. The two alignment possibilities were defined as follows: inwards/outwards-rotational adjustment (I/O-RA) in the transverse plane as δ and varus/valgus adjustment (VR/VL-A) in the frontal plane as ϵ . This is illustrated in Figure 5. The results for the deviations in the frontal ($\sigma_{\text{FKM}}(t)$) and transverse ($\tau_{\text{FKM}}(t)$) plane from equation (5) and (6) will be fitted with the deviations measured during the experiment ($\sigma_{\text{meas}}(t)$, $\tau_{\text{meas}}(t)$). In detail, for each measured and included step of the experiment, the estimated deviations will be compared to the measured deviations of each swing phase over time. Both comparisons, in the frontal and the transverse plane, will be combined in one equation J (see equation (7)). The value of J is calculated with the approach of the minimal squared error with N being the number of measurement points for one swing. Having extracted the minimum of J over the period of time of one swing T , also the best fit of $\sigma_{\text{FKM}}(t)$

and $\tau_{\text{FKM}}(t)$ to the measured data are known. Therefore, the corresponding δ_{est} and ϵ_{est} can be calculated as

$$J = \frac{1}{N} \sum_{n=1}^N \| {}^{\mathcal{W}}\sigma_{\text{FKM}}(\alpha(t), \beta(t), \gamma(t), \eta(t), \delta, \epsilon) - {}^{\mathcal{W}}\sigma_{\text{meas}}(t) \|^2 + \| {}^{\mathcal{W}}\tau_{\text{FKM}}(\alpha(t), \beta(t), \gamma(t), \eta(t), \delta, \epsilon) - {}^{\mathcal{W}}\tau_{\text{meas}}(t) \|^2, \quad (7)$$

$$\min \frac{1}{T} \sum_{t=1}^T J \text{ over } \delta, \epsilon [-10^\circ, 10^\circ].$$

This optimisation for δ and ϵ is done in one iteration for the three middle steps of the trial and averaged to δ_{est} and ϵ_{est} . These results will serve as an estimation for the alignment of the prosthetic knee during the trial. Therewith, we can investigate if we can actually predict the movement of the shank with the known alignment changes.

B. Calculation of adjustment setting for optimal swing

After estimating the real prosthetic alignment (Step 2a), the momentary optimal alignment has to be calculated (Step 2b) to be able to compare them and propose an adjustment in the alignment setting (Step 3). The momentary optimal alignment is defined as the alignment in the knee adapter which would make the shank swing parallel to the PoWD. It is solely dependant on the momentary hip movement and knee flexion of the patient and does not take the measured deviations $\sigma_{\text{meas}}(t)$ and $\tau_{\text{meas}}(t)$ into account. The emphasis is on momentary because the patient is probably using some kind of coping mechanism in the hip due to the alignment not being perfect [2], [8].

With the measured hip movement, the corresponding possible deviations can be calculated with equations (3)-(6). Another approach of the minimal squared error as in equation (7), only regarding the calculated reference values of $\sigma_{\text{FKM}}(t)$ and $\tau_{\text{FKM}}(t)$, like

$$J_{\text{opt}} = \frac{1}{N} \sum_{n=1}^N \| {}^{\mathcal{W}}\sigma_{\text{FKM}}(\alpha(t), \beta(t), \gamma(t), \eta(t), \delta, \epsilon) \|^2 + \| {}^{\mathcal{W}}\tau_{\text{FKM}}(\alpha(t), \beta(t), \gamma(t), \eta(t), \delta, \epsilon) \|^2, \quad (8)$$

$$\min \frac{1}{T} \sum_{t=1}^T J \text{ over } \delta, \epsilon [-10^\circ, 10^\circ],$$

leads to the corresponding optimal value for δ_{opt} and ϵ_{opt} .

IV. ADJUSTMENT PROPOSITION

With the completion of Step 1 and 2, as illustrated in Figure 3, the last missing part is the proposal of alignment adjustments for optimal gait. To calculate the proposed momentary alignment change in Step 3, the difference between the estimated and the optimal angles is taken for δ and ϵ respectively with

$$\delta_{\text{prop}} = \delta_{\text{opt}} - \delta_{\text{est}} \quad \text{and} \quad (9)$$

$$\epsilon_{\text{prop}} = \epsilon_{\text{opt}} - \epsilon_{\text{est}}. \quad (10)$$

This represents the proposed change which the CPO should adjust in the alignment setting of the patient. Positive and

negative signs indicate the direction of change as defined in Figure 5.

V. EXPERIMENTAL PROTOCOL AND DATA ACQUISITION

To obtain data for the inverse kinematic modelling, an alignment session with one amputee was scheduled. The data used in this study was collected from a male above-knee amputee, middle-aged, active and established user of his prosthetic leg. He was amputated on the left side. The participant signed an informed consent form that had been approved by the Human Research Committee from the TU Delft. It can be found in Appendix J.

To collect data, the amputee was equipped with six wireless inertial motion tracking sensors. The sensors were attached with velcro straps to the lower body. One sensor was placed on the shank of the prosthetic, one on the socket, two on shank and thigh of the sound leg and the last two on each side of the hip. Equipped with the sensors, a pre-test was conducted to ensure that the attachment systems were not hindering the participant in any way during walking. The further calculations of this study apply data of the two lower sensors on the prosthetic side. For easy distinction between the sensors on the socket and the prosthetic leg, from now on they will be called thigh-sensor and shank-sensor. Data of the residual sensors was collected and stored for back-up.

For the sensor-body calibration, two positions were measured before each walking trial. The participant was first asked to stand still and then to sit down on a chair with the legs up on another chair. He was asked to keep his toes pointed vertically up. This arrangement is illustrated in Figure 7.

Afterwards, the first walking trial was conducted in a straight line, on level ground at a self selected speed over a distance of 12 meter. From there on, before each next walking trial, the I/O-RA in the transverse plane or the VR/VL-A in the frontal plane was changed and documented. The alignment was modified by an experienced Certified Prosthetist/Orthotist (CPO) and was documented by the researchers. The method for measuring the alignment changed and how they were conducted is explained in Appendix C. The I/O-RA was positive for the inwards and negative for the outwards rotation. Data for the I/O-RA was documented for a range from -10 to $+5$ degrees. The VR/VL-A was positive for the varus and negative

for the valgus tilt. Data for the VR/VL-A was documented for a range from -4.5 to $+3$ degrees. The alignment for the first trial was the one the users walked and lived with in daily life. This was defined as the initial alignment for the measurement of the alignment changes during the trials.

The data was collected from six IMUs from Xsens. They are part of the Xsens MTw Awinda series. They are small and lightweight wireless inertial-magnetic motion trackers for kinematic applications in 3D. The battery powered sensors are 47 mm x 30 mm x 13 mm in size and have a weight of 16 g. The kinematics are tracked with a 3D rate gyroscope and a 3D accelerometer. In addition, the sensors are equipped with a 3D magnetometer, a barometer, and a thermometer. The accelerometer and gyroscope data is captured at a sampling frequency of 1000Hz and is low-pass filtered at a bandwidth of 184Hz. An algorithm then processes the signals into the outputs for orientation and velocity increments.

The orientation is calculated with data from the magnetometer as the movement of the sensor frame in a fixed global frame, which is oriented with a vertical axis up and one axis pointing towards the local magnetic north. Combining the raw acceleration and velocity data with the orientation data, the acceleration and velocity data can be rotated to the fixed global frame [18]. The output frame rate is selectable by the user, dependent on the number of sensors in use, and was set at the recommended rate of 100 Hz for this project.

The data is bundled into packets for each new measurement and stored into a new file for each sensor individually. In the case of using six sensors, there are a total of six new files for each new alignment configuration walk.

VI. DATA PROCESSING

For the purpose of this study, the orientation data output was set to rotational matrices. Xsens provides the orientation data from each sensor frame S to global frame \mathcal{G} , which is fixed in space with respect to the local magnetic north. The velocity as well as the acceleration are provided in each local sensor frame S . The connection between the sensors and the bodies is assumed to be rigid. This means that the the orientation of the thigh and shank-sensor frames is assumed constant with respect to body frames \mathcal{T} and \mathcal{B} , respectively. To obtain necessary input for the kinematic mapping, several measures were taken to prepare the raw data. The following section will explain how the movement of the bodies (thigh and shank) are expressed in the FoWD \mathcal{W} . The frames with respect to each other are illustrated in Figure 8. A summary of the frames can be found in table I in subsection II-B.

First, the X axis of frame \mathcal{W} had to be identified in relation to the $x^{\mathcal{G}}$ axis of frame \mathcal{G} . This was done for both the thigh-sensor and the shank-sensor. Per definition of frame \mathcal{W} (see section II), its X axis points towards the walking direction in the horizontal plane. The horizontal plane could already be found by rotating all of the sensor data into global frame \mathcal{G} . The $z^{\mathcal{G}}$ axis of frame \mathcal{G} and the Y axis of frame \mathcal{W} both point vertically up. Therefore, both the acceleration and the velocity data were referenced in frame \mathcal{G} .

With the vertical axes in line, the last needed rotation to have

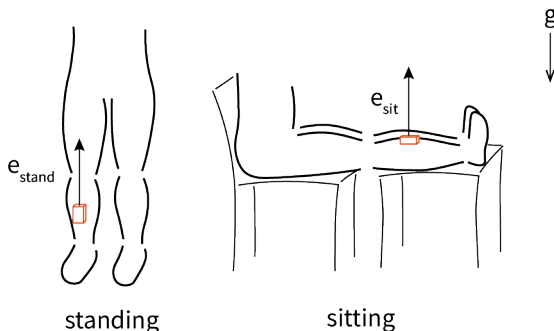


Fig. 7: Standing/sitting calibration for the sensor-body calibration, further explained in appendix C.

X point in the walking direction was around the vertical axis. To identify the walking direction, a principal component analysis (PCA) [19], [20], [21], with the acceleration data in the horizontal plane was conducted as proposed in [22]. The first calculated coefficient served as the X axis of frame \mathcal{W} , and the second as the horizontal Z axis. With this information, a rotation matrix was formed to rotate the sensor data from frame \mathcal{S} to frame \mathcal{W} . More about this process can be found in Appendix D.

With the above mentioned measures, the data shows the movement of both sensors in the FoWD, but not the movement of the bodies of the thigh and the shank themselves. Assuming the sensors will never be perfectly positioned, having the sensor axis S_z pointing in the walking direction (see Figure 4 and 8), the frames for body and sensor would not be the same. Therefore, for instance for the shank-sensor, the data needs to be rotated from sensor frame $\mathcal{S}_{\text{shank}}$ to body frame of the shank \mathcal{B} . Both frames, with respect to each other while standing, are shown in Figure 8. To identify frame \mathcal{B} , the sitting and standing calibration, described in section V was used. With the use of the acceleration vector countering the G-force, each calibration position calculation for the shank-sensor leads to one vector. With those two vectors, the rotation matrix ${}^{\mathcal{S}_{\text{shank}}}\mathbf{R}_{\mathcal{B}}$ can be calculated. Now, the final rotational matrix ${}^{\mathcal{W}}\mathbf{R}_{\mathcal{B}}$ can be formed to track the movement of the shank in the FoWD \mathcal{W} . The same process needs to be applied for the rotation between the thigh-sensor frame $\mathcal{S}_{\text{thigh}}$ and the body frame of the thigh \mathcal{T} .

More information about this process can be found in appendix E. The rotational matrices displaying the orientation were converted into Euler angles with the sequence X-Y-Z. Xsens uses this sequence to calculate the Euler angle orientation output [23] and it is the only sequence that eliminates cross-overs from $+180$ deg to -180 deg. The kinematic mapping only regards the swing phase of the prosthetic leg. Therefore, the respective phases in the measurement data had to be found. The required data extraction followed the descriptions in [24] and is further explained in appendix F. To exclude the influence of acceleration and braking, only the

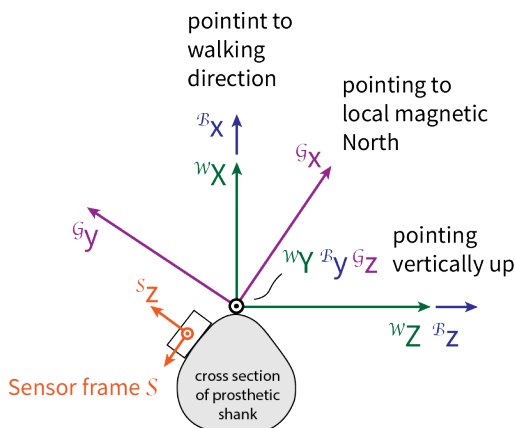


Fig. 8: Frames \mathcal{W} , \mathcal{G} , \mathcal{B} and \mathcal{S} with respect to each other, with cross section through prosthetic shank while standing upright; seen in transverse plane

three middle steps of a walking trial were taken into account for the inverse kinematic mapping in chapter III.

VII. SENSITIVITY ANALYSIS OF KINEMATIC MAPPING

Two sensitivity analyses were performed, to detect how the results are influenced by different parts of the mapping. The inverse kinematic mapping, explained in section III, is dependant on the input of the hip movement, the knee flexion and the deviations of the shank from the PoWD. In the beginning, attempting to only apply the data of the shank-sensor, the hip movement and knee flexion were taken from external sources [25], [26]. How the data was collected is explained in appendix A. It is known, however, that amputees adapt to changes in the alignment of their prosthetic knee and change their movement pattern of the hip accordingly [2], [8]. Therefore, it was assumed, that the hip movement of the amputees might deviate greatly from the movement obtained by [25] and in addition changes with every alignment adjustment in the prosthetic knee. Thus, a sensitivity analysis was performed on the input data of the hip movement to identify the importance of the hip movement for the final results.

As a basis for the second sensitivity analysis, the estimation of the sensor placement with respect to the body was identified as a weak point in the kinematic mapping. This includes the orientation of the thigh-sensor with respect to the thigh as well as the orientation of the shank-sensor with respect to the shank. This obstacle follows the assumption, that the calibration with sitting and standing positions might not be accurate enough. Especially in the sitting position, asking the participants to point their feet up might not be a reliable instruction. One one hand, the foot had to be rotated if an inwards/outwards rotational adjustment was conducted, to have it point in the right direction. On the other hand, the participants constantly forgot to make sure to point their feet up. Both could have lead to errors.

A sensitivity analysis is performed on the rotation matrix between the shank and the shank-sensor ${}^{\mathcal{S}_{\text{shank}}}\mathbf{R}_{\mathcal{B}}$. Therefore, an additional disturbed frame, $\hat{\mathcal{B}}$, is introduced. This biased body frame is rotated individually around x^{VI} , y^{VI} and z^{VI} by ± 5 degrees with respect to body frame \mathcal{B} . The procedure is explained in detail in appendix H. The artificial disturbances take effect on Step 1a of the calculation towards an algorithm, illustrated in Figure 3. With a rotation matrix between the sensor and the biased body frame $\hat{\mathcal{B}}$ instead of the body frame \mathcal{B} , the inverse kinematic mapping is performed as described in chapter III. The end result of the disturbed adjustment angles $\hat{\delta}$ and $\hat{\epsilon}$ are used to calculate a one-at-a-time sensitivity analysis depending on the rotation around the single axis.

Sensitivity of the sensor-body calibration Sensitivity_{SB} is calculated separately for δ and ϵ according to the following formulas

$$\text{Sensitivity}_{SB,\delta} = \delta_{\text{est}} - \hat{\delta}, \quad (11)$$

$$\text{Sensitivity}_{SB,\epsilon} = \epsilon_{\text{est}} - \hat{\epsilon}. \quad (12)$$

δ_{est} and ϵ_{est} are the calculated adjustment angles obtained with the measurement input (Step 2a), explained in chapter III. $\hat{\delta}$ and $\hat{\epsilon}$ are the resulting disturbed adjustment angles calculated with the biased sensor-body rotation matrix ${}^{\mathcal{S}_{\text{shank}}}\mathbf{R}_{\hat{\beta}}$.

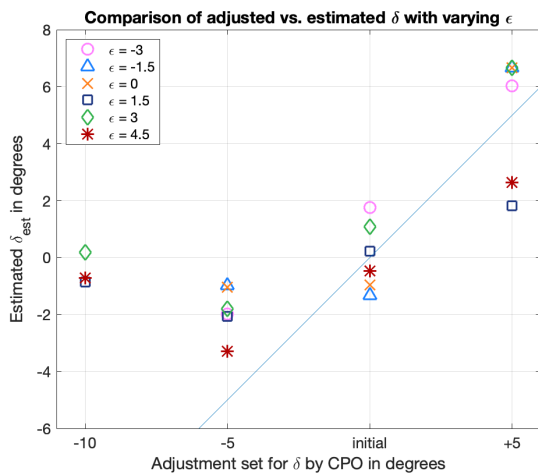
VIII. RESULTS

A. Evaluation of mapping

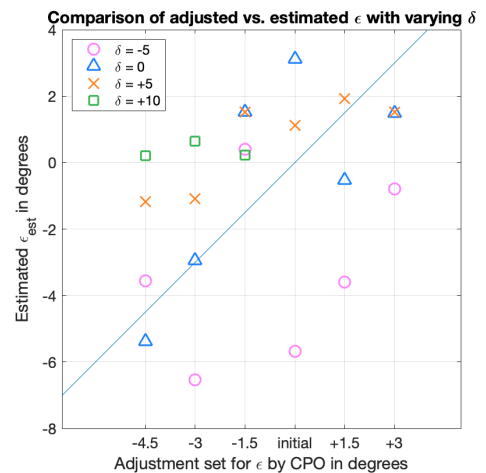
After the processing, discussed in section VI, the data from the shank and the thigh sensor of the prosthetic side was fed into the inverse kinematic mapping, as described in chapter III. The expectation was, that the estimation results for δ and ϵ from the inverse mapping (Step 2a) coincide with the actual adjusted angles in the experiments. This would lead to a linear trend with slope 1, shown as the blue line in each plot.

Both adjustments I/O-RA and the VR/VL-A influence the movement of the shank and the measured deviations $\sigma(t)$ and $\tau(t)$. However, as it is difficult to analyse them simultaneously, the results will be looked at one-by-one. For example, Figure 9a displays the results for I/O-RA angle δ for the first participant. The results for δ are grouped by alignment changes of $[-10; 5]$ degrees, within these groups are the δ results for changes of the VR/VL-A angle ϵ of $[-4.5; 3]$ degrees. The used values of ϵ are distinguished with different markers, which are shown in the legend of the plot. The actual experiment adjustments are shown on the horizontal axis and the resulting estimated δ_{est} from the inverse kinematic mapping on the vertical axis. With exception of the group at the experimental adjustment of -10 degrees, the data is following a linear trend.

The results for ϵ , displayed in Figure 9a are grouped by changes of $[-4.5; 3]$ degrees with therein changing δ of $[-10; 5]$ degrees. Again, the used values of δ are distinguished with different markers, which are shown in the legend of the plot. The weak linear trend between the experimental adjustment on the horizontal and the resulting estimations on the vertical axis can be seen.



(a) Estimated δ_{est} , grouped for various ϵ



(b) Estimated ϵ_{est} , grouped for various δ

Fig. 9: Estimated alignment angles δ_{est} and ϵ_{est} in prosthetic knee

The results of the desired momentary optimal alignment settings (Step 2b) are illustrated in Figure 10. Like the results for the estimated adjustment angles, for each angle the results are shown in groups of the other variable angle. The results were expected to be around the same value, as there is only one optimal alignment setting for each patient [8]. However, amputees adapt their hip movement when the alignment is not optimal to get the most comfortable walk. As those adaptation movements influence the calculations, deviations were expected. The results for δ_{opt} show an accumulation of the data points around 0 till -2 degrees (shown with the blue lines in Figure 10a) with far outliers for the group of δ being set at -5 degrees. The results for ϵ_{opt} accumulate around the area of 0 and 2 degrees (shown with the blue lines in Figure 10b). It shows three big outliers, which are all from the group of adjusted δ for -5 degrees, represented as circles.

B. Adjustment proposition

With equations (9) and (10), the proposed changes in δ_{prop} and ϵ_{prop} could be calculated. They are shown in Figure 11. The x-axis of Figure 11a shows the actual adjustment from the initial alignment for δ . Again, these are groupings of varying ϵ . The y-axis shows the momentary proposed alignment changes to get an optimal swing.

Figure 11b shows the same concept for ϵ with groups of varying δ . A table with the adjusted alignments, the estimated alignments, the estimated optimal alignments and the proposed changes is displayed in appendix I.

The data is showing a linear trend with a slight positive slope for δ and a negative slope for ϵ .

C. Sensitivity

Both sensitivity analyses were done for one walking trial. The chosen trial for this analysis was with the optimal alignment ². Early on, the sensitivity analysis on the external

² The optimal alignment in this case being decided by the CPO in consultation with the patient.

hip movement data input was performed. It showed that a small bias on the hip movement had a big influence on the estimation results for δ and ϵ . The biggest influences came from disturbances in the hip rotation $\alpha(t)$ and the abduction $\beta(t)$. This part of the sensitivity analysis is to be found in appendix G. As it is further known that amputees adapt strongly to different alignments, it was decided that the external input was not realistic enough for our cause and the input procedure was changed. The real hip movement of the patient, measured with the inertial sensors, was used as the input for the kinematic mapping. All the results in section VIII-A were obtained with the data from both thigh and shank-sensor, as explained in section VI. Therefore, any adaptation in the hip was included in the forward and the inverse mapping and does not have an additional influence on the outcome.

The sensitivity analysis on the sensor-body orientation was performed with the use of a biased body frame replacing the calculated body frame. \hat{B} is rotated ± 5 around all three axes of frame B . Those rotations are done one-by-one, to see the influence each axis rotation has. The calculation of frame B is based on the standing/sitting calibration described in appendix E. Bias in the different axis rotations could in reality be based on an ab-/adduction during standing for a rotation around the x axis, standing too far on the toes/heels for a rotation around the y axis or having the feet not pointing vertically up for a rotation around the z axis.

With the introduction of frame \hat{B} , the rotation matrix between sensor and biased body is changed to ${}^S\mathbf{R}_{\hat{B}}$ and therefore between the FoWD and biased body to ${}^W\mathbf{R}_{\hat{B}}$. The newly calculated Euler angles of the movement of the shank around the different axis with bias in the sensor-body rotation are to be found in Appendix H.

As the sequence to convert the rotational matrices to Euler angles was chosen to be X-Y-Z, the biases on the singular axis rotations carry different weight on the offset of the orientation. A bias on the rotation around the x axis

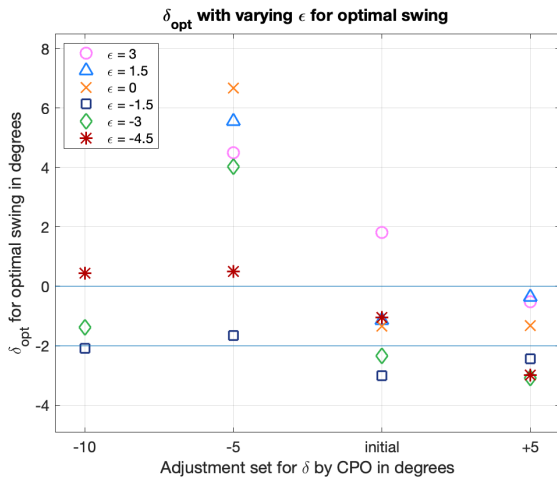
influences the orientation of all Euler angles around the x , y and z axis. A bias on the rotation around the z axis has no effect on the orientation of the Euler angles around the x and y axis. However, if the resulting disturbed alignment angles $\hat{\delta}$ and $\hat{\epsilon}$ are compared, there are still differences to be seen in the bias on the rotation around the z axis. This is due to the fact that the inverse kinematic mapping includes both deviations $\sigma(t)$ and $\tau(t)$ in the fitting, where $\sigma(t)$ is represented by the rotation around the x axis and $\tau(t)$ by the rotation around the z axis. If e.g. only $\sigma(t)$ was regarded in the fitting process, the results on the alignment estimations would not change with a bias around the z axis in the sensor-body orientation. All of the results are to be found in table IV in appendix H. Figures 12a and 12b display the results for $\hat{\delta}$ and $\hat{\epsilon}$ as deviations from the original value, shown in the horizontal line.

IX. DISCUSSION

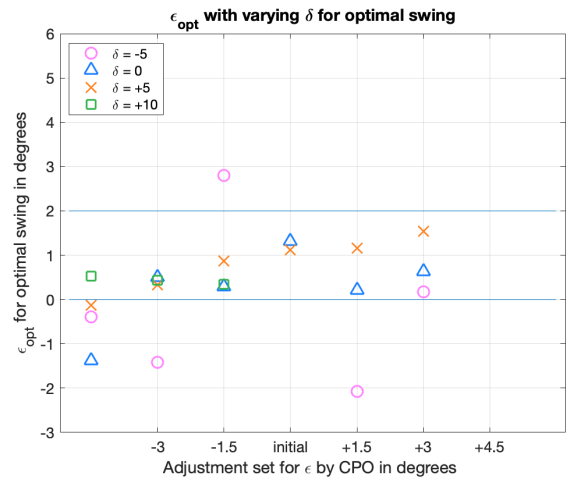
A. Kinematic mapping

The first part of this study was to see if we were able to estimate which alignment was set in a prosthetic knee in the frontal and transverse plane at the moment of use (Step 2a). With this information and the calculation of the optimal setting (Step 2b) we hoped to be able to give recommendations on how to change the alignment to achieve a smooth gait pattern for the patient (Step 3). The results discussed in subsection VIII-A focus on the results of Step 2: Inverse kinematic mapping, as illustrated in Figure 3. For the results of Step 2a, the estimation of δ and ϵ in Figure 9, we would have expected a linear trend with the slope of 1. If the adjustment setting of one of the angles was changed by the CPO by 5 degrees, we also expected an offset of the estimated angle by 5 degrees.

The results for the estimation of the I/O-RA angle δ_{est} in Figure 9a partly show an accumulation of the data points around a linear trend in between the alignment settings by the CPO of



(a) Desired δ_{opt} , grouped for various ϵ



(b) Desired ϵ_{opt} , grouped for various δ

Fig. 10: Desired alignment angles δ_{opt} and ϵ_{opt} for optimal swing

-5 till $+5$ degrees. The linear trend with slope 1 is shown with the blue line. The difference in the slope could be explained by errors in the data processing, by an incorrect estimation of the walking direction or by disturbances in the sensor-body orientation (see the discussion of the sensitivity analysis in section IX-C).

The group of data points when δ was adjusted to -10 degrees shows a big offset. There could be several explanations for this. A part of the offset could be justified by a measurement error while setting the new alignment by the CPO. There were problems with the measurement disk, described in Appendix C. It was noticed that once turned back to the initial alignment, the marker on the disk showed not the expected zero position. This error occurred only during the end, when measurements with δ at -10 degrees were done. Unfortunately the awareness about the error only came after these measurements were finished. Furthermore, the participant was walking very unstable with δ being set at -10 degrees. A clear lack of balance and a swaying gait were witnessed by the researchers. The origin of the estimation error could be that the patient compensated with adapted movement of the pelvis, which is not taken into account in the calculations. If this assumption is correct, it rises the question for which range of alignment angles the proposed estimation can be accurate.

The results for the estimation of the VR/VL-A angle ϵ_{est} show a weak accumulation around a linear trend with the slope of 1, which is shown in the blue line in Figure 9b. Some of the groups assorted by different alignment settings of δ show a linear tendency, however, always with outliers. The group of ϵ_{est} with a set δ of -5 degrees for example shows a linear tendency with an offset of around 4 degrees with one outlier for ϵ of -1.5 and one for -4.5 degrees. One explanation for the results not having the linear trend we expected could lie in the results of the sensitivity analysis of the sensor-body orientation. They show that the adjustment angle ϵ is more sensitive to disturbances in the sensor-body orientation than the adjustment angle δ . Therefore, errors in the sensor-body

orientation could be a cause for offsets and outliers in the estimation of ϵ .

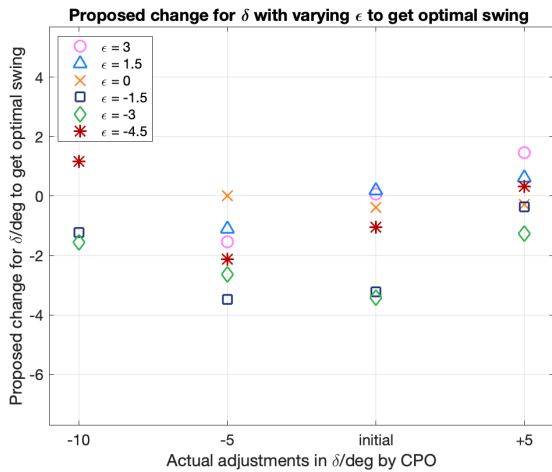
The results for Step 2b, the calculation of the desired adjustment setting for optimal swing, are shown in Figure 10. The desired optimum is calculated with the results of the forward kinematic mapping $\sigma_{\text{FKM}}(t)$ and $\tau_{\text{FKM}}(t)$ which include hip movement and knee flexion from the sensors. Ideally, the results should have all shown the same value, as there is only one optimal alignment setting for each patient [8]. Deviations were expected though, produced by hip adaptation movement of the participant [2], [8].

Both plots show a rough accumulation of data points around one value. The outliers in the results for δ_{opt} mostly lie the group of δ being set at -5 degrees. In combination with the three biggest outliers for ϵ_{opt} , which are also from the group of adjusted δ for -5 degrees, the assumption arises, that the participant was least comfortable with the alignment setting of -5 degrees for δ , with the consequence of bigger hip adaptation movement.

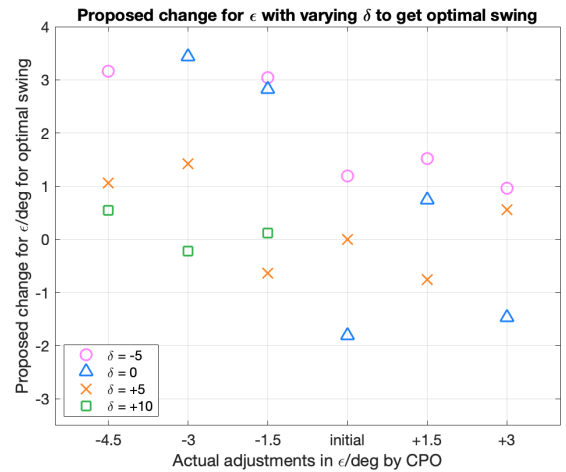
B. Adjustment proposition

The results for δ_{prop} , ϵ_{prop} also show a linear trend. The expectation for these results also was a linear trend, however with the slope of -1 , as the proposed alignment changes should change inversely correlated to the adjustment changes made. The results for ϵ_{prop} show the expectations nicely with a slope around -1 . The results for δ_{prop} , however, resemble more the results of δ_{est} . This can be explained by the outliers in the results of δ_{opt} , which are mentioned above.

There was hope that the deviations in the calculation of the estimated angles δ_{est} , ϵ_{est} and the deviations in the calculation for the desired optimal angles δ_{opt} , ϵ_{opt} would cancel each other out. That could have lead to a more steady change proposal in δ_{prop} , ϵ_{prop} . This would have for example been the case if during the data processing, the same wrong orientation or heading was assumed for both of them. The data, however, shows otherwise. This leads to the conclusion that there are



(a) Adjustment propositions δ_{prop} , grouped for various ϵ



(b) Adjustment propositions ϵ_{prop} , grouped for various δ

Fig. 11: Adjustment propositions δ_{prop} and ϵ_{prop} for the knee adapter alignment angles δ and ϵ

more influences that were not yet regarded in this work.

C. Sensitivity analysis

The sensitivity analysis of the sensor-body orientation investigated the result of disturbances in the rotational matrices in Step 1a onto the estimation of the alignment angles. In the resulting disturbed $\hat{\delta}$ from Step 2a, the most sensitive rotations for a ± 5 degree disturbance in the sensor-body estimation, are the ones around the x and z axis with an induced disturbance of around ± 1 degrees. For $\hat{\epsilon}$, the most sensitive axis is the x axis with a resulting error of around ± 2 degrees, followed by the z axis with a resulting error of around ± 1 degree.

Both alignment angles are sensitive for disturbances in the estimation of the sensor-body orientation in the x and z axis. With the x axis being estimated with the standing, and the z axis with the sitting position, the whole calibration process has to be precise. In practice, the biggest error is probably induced with the sitting calibration. If the participant does not make sure to keep the feet pointed up vertically, both estimation angles will be assumed wrong.

The pointing up of the feet could have additionally be influenced. When the I/O-RA angle was changed, the foot was rotated the opposite direction to have it point forward again during stance. However, the CPO was not able to do this rotation very precisely. So even if the participant tried to have the feet point up, there could still be an error due to an error in the correction rotation of the feet. This could in addition explain the whole group of outliers for results of I/O-RA angle δ for the alignment angle of -10 degrees.

An additional rotation between the sensor and the body frame was expected to have the same effect as the rotation of the prosthesis. Therefore, also in the resulting alignment angles $\hat{\delta}$ and $\hat{\epsilon}$ of the sensitivity analysis, a linear trend with the slope of 1 was expected. The linear trend can clearly be seen in Figure 12. However, the slope in both plots is smaller than

1. Part of this is probably caused by the fact that the fitting in Step 2, the inverse kinematic mapping, is done with a combination of $\sigma(t)$ and $\tau(t)$ and further over δ and ϵ at the same time. However, it also indicates that there are additional influences that have not been regarded yet. For example is it possible that the orientation of the adapter on the prosthetic socket (in more detail in Appendix B) plays a bigger role than expected.

D. General

The sensitivity analysis of the sensor-body orientation shows, that a more robust way has to be found to estimate the relation between those frames. Another approach was tested but discarded. For that approach, it was assumed that while standing upright, FoWD \mathcal{W} and shank-fixed frame \mathcal{B} are in line and therefore equal. With use of the orientation of the sensor in the \mathcal{W} frame during stance, the final rotational matrix ${}^{\mathcal{W}}\mathbf{R}_{\mathcal{B}}$ could be formed. However, it was not possible to find the exact moment during the stance phase were the participant was standing exactly upright.

Moreover, a more precise way to define the walking direction has to be determined. The calculation with a PCA of the acceleration, as it was done in this paper, is too prone to errors. Every PCA could have a mean error of 5 degrees, as described in [22]. With a PCA with the data of the thigh-sensor and the shank-sensor, this can accumulate to an error up to 10 degrees.

Apart from the one mentioned experimental set-up, there was one more trial done with another male, middle-aged participant, also amputated on the left side. However, the measured data appears to be faulty. Due to lack of time, it could not be investigated, where the errors were based on. As it was a different day for the experiments, it is possible that the magnetic surroundings changed. The data could have, for example, been influenced by the turning on and off of a nearby machine that created a magnetic field. Another

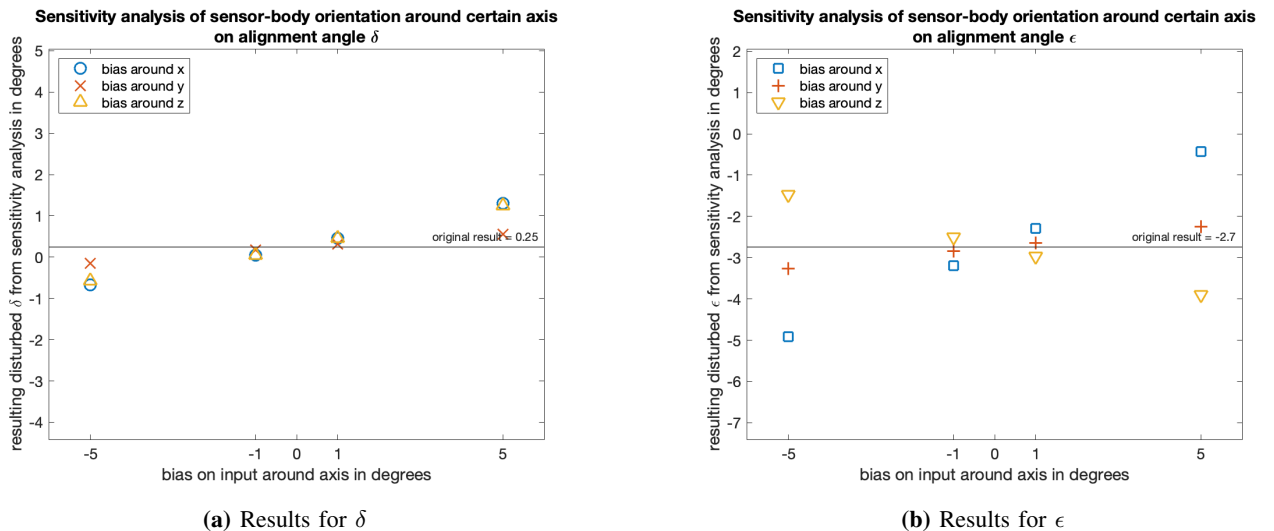


Fig. 12: Results of the sensitivity analysis of the sensor-body orientation on the estimation of the alignment angles δ and ϵ

possibility is that the connection of the sensors to the body of the participant was not fully rigid. Finally, the participant received a new prosthetic knee right before the experiment was conducted. It is possible, that changes in the sagittal alignment or a different controlling system influenced the patients walking pattern during the experiment. The results for δ_{est} and ϵ_{est} as results of Step 2a for the second trial are included in Appendix I.

Concluding, the results of the estimation for both adjustment angles leave room for questions. It would be beneficial, if an estimation of the walking direction could be done without the use of the sensor magnetometer data. It is known that those measurements are prone to magnetic distortions. The area where the measurements took place was not mapped for those. Additionally, the prosthesis in the tests was equipped with electro-motors that execute the swing of the leg. During walking, an algorithm in the sensors filters those distortions but it is not known in detail, how it is implemented by the provider of the sensors and if there could be a residual error. This point will have to be considered for future measurements.

X. CONCLUSION

The goal of this work was to predict the alignment settings at the moment of measurement and therewith identify the changes that should be made to achieve a parallel swing. To survey how well the results are aligned with the goal, the inverse kinematic mapping in Step 2, as illustrated in Figure 3, was reviewed for accuracy. The results show a promising trend towards linearity with the slope of 1. However, there are still deviations that have to be examined.

Most uncertainty in the algorithm lies in the preparation of the sensor data, because it is implemented in every step of the process. Therein lie several possible sources of error. They can have their origin in the PCA for the walking direction estimation or in the assumption that all frames are in line while standing upright. As the sensitivity analysis shows, they can also descend from the sensor-body orientation estimation. Small errors in each step could account for the deviations that are detected. Alone the combined PCAs could be the origin of an error up to 10 degrees. The approach to eliminate those uncertainties would be to either reduce the errors in every step of the data processing or to choose replacement steps with a smaller to non-existent error margin.

One possible approach to reduce errors would be to conduct a sensor fusion between the thigh and the shank sensor over

one rotation axis [27]. This is feasible as a prosthetic knees only has one degree of freedom, the flexion and extension. Another approach could be to recalibrate the orientation of the sensors to each other with every step. To find, for example, the upright standing part of the stance phase, a sensor on the foot instead of the shank could be utilised [28]. Both approaches could be supported by selected filtering [28], [29].

Another possible influence that was found but not further investigated is an influence of the sensor-body orientation on the extraction of the individual swing phases. The reason is, that the key-events used for the step division (approach explained in F) are influenced by the way the sensor-body orientation is done. This influence could not be further analysed as part of this research and is presented as a possibility for future work. Other suggestions for future work include research into the quality of the steps the participant took. This goes from checking if the steps were sufficiently completed (no stumble, no breaking) until examining if the person was walking straight.

As it was only possible for us to evaluate Step 2 of the model, the inverse fitting, another method of validation should be incorporated. To prove that the presented approach is successful and to examine the accuracy of every step of the way, the research of the IMU data could be combined with recordings from a motion capture system.

The work on hand lies out the basis towards a simple way of achieving the optimal knee alignment for femoral amputees in the frontal and transverse plane. Once the known and unknown factors above are eliminated we are sure that the goal of recommending alignment changes for a smoother gait is within reach. It can further contribute to computer simulation, demonstration in teaching, visual feedback and training purposes.

ACKNOWLEDGEMENTS

I would like to thank my Master Thesis supervisors, namely Herman Boiten, Heike Vallery, Manon Kok and Gerwin Smit for all their helpful insights, comments and time. For his time and patience during the experiments, I want to thank Dries Glorieux. Further, I want to thank the members of the Biorobotics Lab at the TU Delft for their support. Special thanks to Patricia Baines, Saher Jabeen and Andrew Berry for their helpful input and endless patience.

REFERENCES

- [1] C. W. Radcliffe, "Functional Considerations in the Fitting of Above-Knee Prostheses," 1955, pp. 35–60.
- [2] S. S. Salgado and A. T. Velásquez, "Analysis of the frontal plane alignment in AK prosthesis," *PAHCE*, pp. 0–4, 2013.
- [3] S. R. Koehler-McNicholas, R. D. Lipschutz, and S. A. Gard, "The biomechanical response of persons with transfemoral amputation to variations in prosthetic knee alignment during level walking," *JRRD*, vol. 53, no. 6, pp. 1089–1106, 2016.
- [4] M. Schaarschmidt, S. W. Lipfert, C. Meier-gratz, H.-c. Scholle, and A. Seyfarth, "Human Movement Science Functional gait asymmetry of unilateral transfemoral amputees," *Human Movement Science*, vol. 31, no. 4, pp. 907–917, 2012. [Online]. Available: <http://dx.doi.org/10.1016/j.humov.2011.09.004>
- [5] R. Gailey, K. Allen, J. Castles, J. Kucharik, and M. Roeder, "Review of secondary physical conditions associated with lower-limb amputation and long-term prosthesis use," *JRRD*, vol. 45, no. 1, pp. 15–30, 2008.
- [6] T. Zhang, X. Bai, F. Liu, and Y. Fan, "Effect of prosthetic alignment on gait and biomechanical loading in individuals with transfemoral amputation: A preliminary study," *Gait and Posture*, vol. 71, no. 37, pp. 219–226, 2019. [Online]. Available: <https://doi.org/10.1016/j.gaitpost.2019.04.026>
- [7] M. S. Zahedi, B. Sc, W. D. Spence, and M. Sc, "Alignment of lower limb prostheses," *Journal of Rehabilitation Research and Development*, vol. 23, no. 2, pp. 2–19, 1986.
- [8] L. Yang, S. E. Solomonidis, W. D. Spence, and J. P. Paul, "The influence of limb alignment on the gait of above-knee amputees," *Journal of Biomechanics*, vol. 24, no. 11, pp. 981–997, 1991.
- [9] M. D. Muller, "Transfemoral Amputation: Prosthetic Management," in *Atlas of Amputations and Limb Deficiencies*, 4th ed. American Academy of Orthopaedic Surgeons, 2016, ch. 46, pp. 537–554.
- [10] M. Bellmann, S. Blumentritt, M. Pusch, T. Schmalz, and M. Schoene-meier, "The 3D L.A.S.A.R. - A New Generation of Static Analysis for Optimising Prosthetic and Orthotic Alignment," *Orthopaedie Technik*, no. 12, pp. 18–25, 2017.
- [11] M. D. Geil, "Variability among Practitioners in Dynamic Observational Alignment of a Transfemoral Prosthesis," *Prosthetic and Orthotic Science*, vol. 14, no. 4, pp. 159–164, 2002.
- [12] S. D. Stulberg, "Computer navigation as a teaching instrument in knee reconstruction surgery," *The journal of knee surgery*, vol. 20, no. 2, pp. 165–172, 2007.
- [13] T. Schmalz, S. Blumentritt, and R. Jarasch, "Energy expenditure and biomechanical characteristics of lower limb amputee gait: The influence of prosthetic alignment and different prosthetic components," *Gait and Posture*, vol. 16, pp. 225–263, 2002.
- [14] T. Kobayashi, M. S. Orendurff, and D. A. Boone, "Dynamic alignment of transtibial prostheses through visualization of socket reaction moments," *Prosthetics and Orthotics International*, vol. 39, no. 6, pp. 512–516, 2015.
- [15] J. Mizrahi, Z. Susak, R. Seliktart, and T. Najenson, "Alignment procedure for the optimal fitting of lower limb prostheses," *Journal of Biomed*, vol. 8, pp. 229–234, 1986.
- [16] M. A. LaFortune, "Three-dimensional kinematics of the human during walking," *Journal of Biomechanics*, vol. 25, no. 4, pp. 347–357, 1992.
- [17] H. Vallery and A. L. Schwab, *Advanced Dynamics*, 2nd ed., P. de Jong, Ed. Technische Universiteit Delft, 2018.
- [18] M. Paulich, M. Schepers, N. Rudigkeit, and G. Bellusci, "Xsens MTw Awinda: Miniature Wireless Inertial-Magnetic Motion Tracker for Highly Accurate 3D Kinematic Applications," pp. 1–9.
- [19] H. Abdi and L. J. Williams, "Principal component analysis," *Wiley Interdisciplinary Reviews: Computational Statistics*, vol. 2, no. 4, pp. 433–459, 2010.
- [20] K. Esbensen and P. Geladi, "Principal Component Analysis," *Chemo-metrics and Intelligent Laboratory Systems*, vol. 2, pp. 37–52, 1987.
- [21] I. Jolliffe, *Principal Component Analysis*, 2nd ed. New York: Springer-Verlag New York, 2002.
- [22] K. Kunze, P. Lukowicz, K. Partridge, and B. Begole, "Which Way Am I Facing: Inferring Horizontal Device Orientation from an Accelerometer Signal Which way am I facing: Inferring horizontal device orientation from an accelerometer signal," *International Symposium on Wearable Computers*, no. October, pp. 2009–2011, 2009.
- [23] "MTw Awinda User Manual," Tech. Rep. Revision L, 2018.
- [24] S. R. Hundza, W. R. Hook, L. Member, C. R. Harris, S. V. Mahajan, P. A. Leslie, C. A. Spani, L. G. Spalteholz, B. J. Birch, D. T. Commanneur, and N. J. Livingston, "Accurate and Reliable Gait Cycle Detection in Parkinson' s Disease," *Transactions on neural systems and rehabilitation engineering*, vol. 22, no. 1, pp. 127–137, 2014.
- [25] B. Koopman, E. H. van Asseldonk, and H. Van der Kooij, "Speed-dependent reference joint trajectory generation for robotic gait support," *Journal of Biomechanics*, vol. 47, no. 6, pp. 1447–1458, 2014. [Online]. Available: <http://dx.doi.org/10.1016/j.jbiomech.2014.01.037>
- [26] J. Rose and J. G. Gamble, *Human Walking*, 3rd ed. Lippincott Williams & Wilkins, 2006.
- [27] P. Picerno, "25 years of lower limb joint kinematics by using inertial and magnetic sensors : A review of methodological approaches," *Gait & Posture*, vol. 51, pp. 239–246, 2017. [Online]. Available: <http://dx.doi.org/10.1016/j.gaitpost.2016.11.008>
- [28] X. Li, Y. Wang, and D. Liu, "Research on Extended Kalman Filter and Particle Filter Combinational Algorithm in UWB and Foot-Mounted IMU Fusion Positioning," *Mobile Information Systems*, vol. 2018, 2018.
- [29] J. A. Zeni, J. G. Richards, and J. S. Higginson, "Two simple methods for determining gait events during treadmill and overground walking using kinematic data," vol. 27, pp. 710–714, 2008.

APPENDIX A
REFERENCE DATA

Koopman et al. [25] designed a method to generate reference joint trajectories based on height and walking speed of the person. The authors provide a MATLAB function in combination with a matrix. The code has the option to integrate the desired height and walking speed of the person that should be referenced. The result is a MATLAB spline that contains data for hip abduction, hip flexion, knee flexion and ankle flexion. The hip abduction is calculated with respect to the pelvis. However, for this thesis, the hip abduction was needed as an orientation in space. Therefore, only hip and knee flexion from [25] were used for the calculation of the hip movement sensitivity in G.

To get a full movement of the hip in 3D, the hip abduction and rotation was taken from [26]. The hip abduction as an orientation in space was acquired by subtracting the pelvic abduction movement from the hip abduction. The hip rotation was used as given.

APPENDIX B
ANGLES, FRAMES AND ROTATIONAL MATRICES FOR
FORWARD MAPPING

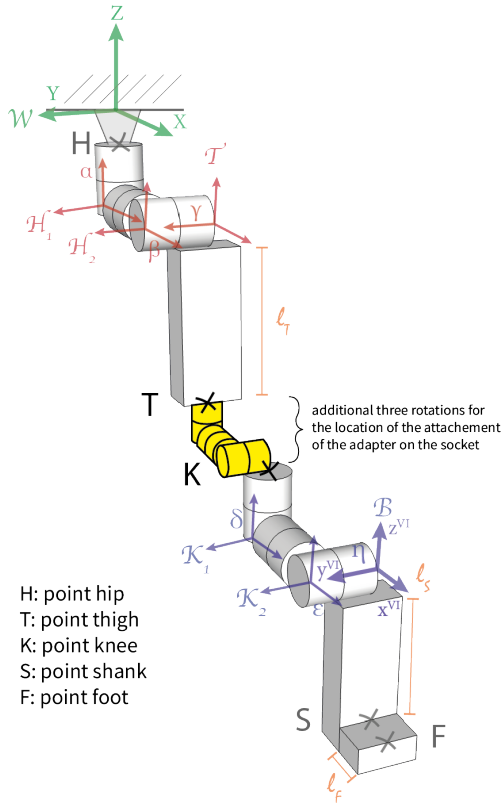


Fig. 13: Illustration of kinematic mapping model with inclusion of possible orientation influence of knee adapter on socket

Figure 13 shows the model for the mapping with the corresponding frames. Contrary to the Figure 4, it includes the disregarded possible influence of the orientation of the

knee adapter on the socket. It is illustrated as additional three rotations between the thigh (point T) and the knee (point K). Therefore, there is a possible difference between frame \mathcal{T} and \mathcal{K}_1 in addition to a rotation around δ .

All frames are associated with a right-handed coordinate system. Frame \mathcal{W} has a vertical Y axis and the X axis pointing towards the walking direction. The first of the continuing six moving frames, \mathcal{H}_1 , rotates with $\alpha(t)$ around the z^I axis. The axes y^I and Y are aligned. The last of the six frames \mathcal{B} is fixed to the shank and rotates with $\eta(t)$ around the z^{VI} axis. The orientation of frames \mathcal{H}_1 , \mathcal{H}_2 and \mathcal{T} represent the hip movement, introduced by angles $\alpha(t)$, $\beta(t)$ and $\gamma(t)$. Frame \mathcal{T} is attached to the body of the thigh. Frames \mathcal{K}_{1-2} represent movements due to the alignment changes in the knee adjustment δ and ϵ . Finally, frame \mathcal{B} is fixed to the body of the shank and is dependant on the knee flexion angle $\eta(t)$. The definition of the angles, their function and allocation with respect to the frames are listed in Table II.

Angle	Function	Frame Rotation
$\alpha(t)$	hip rotation	\mathcal{W} to \mathcal{H}_1
$\beta(t)$	hip abduction	\mathcal{H}_1 to \mathcal{H}_2
$\gamma(t)$	hip flexion	\mathcal{H}_2 to \mathcal{T}
δ	knee rotation	\mathcal{T} to \mathcal{K}_1
ϵ	knee abduction	\mathcal{K}_1 to \mathcal{K}_2
$\eta(t)$	knee flexion	\mathcal{K}_2 to \mathcal{B}

TABLE II: Definition, function and allocation of angles

The zero position for all angles is defined by the upright standing position with the toes pointing towards forward. In this position, all frames are aligned with the FoWD. The single rotations from each frame to the next, as introduced in Figure 13 are defined as

$$\mathcal{W}\mathbf{R}_{\mathcal{H}_1}(t) = \begin{bmatrix} \cos \alpha(t) & 0 & \sin \alpha(t) \\ 0 & 1 & 0 \\ -\sin \alpha(t) & 0 & \cos \alpha(t) \end{bmatrix}, \quad (13)$$

$$\mathcal{H}_1\mathbf{R}_{\mathcal{H}_2}(t) = \begin{bmatrix} 1 & 0 & 0 \\ 0 & \cos \beta(t) & -\sin \beta(t) \\ 0 & \sin \beta(t) & \cos \beta(t) \end{bmatrix}, \quad (14)$$

$$\mathcal{H}_2\mathbf{R}_{\mathcal{T}}(t) = \begin{bmatrix} \cos \gamma(t) & -\sin \gamma(t) & 0 \\ \sin \gamma(t) & \cos \gamma(t) & 0 \\ 0 & 0 & 1 \end{bmatrix}, \quad (15)$$

$$\mathcal{T}\mathbf{R}_{\mathcal{K}_1}(t) = \begin{bmatrix} \cos \delta & 0 & \sin \delta \\ 0 & 1 & 0 \\ -\sin \delta & 0 & \cos \delta \end{bmatrix}, \quad (16)$$

$$\mathcal{K}_1\mathbf{R}_{\mathcal{K}_2}(t) = \begin{bmatrix} 1 & 0 & 0 \\ 0 & \cos \epsilon & -\sin \epsilon \\ 0 & \sin \epsilon & \cos \epsilon \end{bmatrix}, \quad (17)$$

$$\mathcal{K}_2\mathbf{R}_{\mathcal{B}}(t) = \begin{bmatrix} \cos \eta(t) & -\sin \eta(t) & 0 \\ \sin \eta(t) & \cos \eta(t) & 0 \\ 0 & 0 & 1 \end{bmatrix}. \quad (18)$$

The combined rotation of the hip movement with respect to the FoWD

$${}^{\mathcal{W}}\mathbf{R}_{\mathcal{T}}(t) = {}^{\mathcal{W}}\mathbf{R}_{\mathcal{H}_1} \cdot {}^{\mathcal{H}_1}\mathbf{R}_{\mathcal{H}_2} \cdot {}^{\mathcal{H}_2}\mathbf{R}_{\mathcal{T}}, \quad (19)$$

and the combined rotation of the knee movement with respect to the thigh

$${}^{\mathcal{K}_3}\mathbf{R}_{\mathcal{B}}(t) = {}^{\mathcal{T}}\mathbf{R}_{\mathcal{K}_1} \cdot {}^{\mathcal{K}_1}\mathbf{R}_{\mathcal{K}_2} \cdot {}^{\mathcal{K}_2}\mathbf{R}_{\mathcal{B}}, \quad (20)$$

lead the rotation of shank-body frame \mathcal{B} respect to the FoWD \mathcal{W} defined as

$${}^{\mathcal{W}}\mathbf{R}_{\mathcal{B}}(t) = {}^{\mathcal{W}}\mathbf{R}_{\mathcal{T}} \cdot {}^{\mathcal{T}}\mathbf{R}_{\mathcal{B}}. \quad (21)$$

With equations (13)-(21) this leads to

$$\begin{aligned} {}^{\mathcal{W}}\mathbf{R}_{\mathcal{B}}(1.1) &= (\mathbf{c}\alpha\mathbf{c}\gamma + \mathbf{s}\alpha\mathbf{s}\beta\mathbf{s}\gamma)(\mathbf{c}\delta\mathbf{c}\eta + \mathbf{s}\delta\mathbf{s}\epsilon\mathbf{s}\eta) \\ &\quad - \mathbf{c}\beta\mathbf{s}\alpha(\mathbf{c}\eta\mathbf{s}\delta - \mathbf{c}\delta\mathbf{s}\epsilon\mathbf{s}\eta) - \mathbf{c}\epsilon\mathbf{s}\eta(\mathbf{c}\alpha\mathbf{s}\gamma - \mathbf{c}\gamma\mathbf{s}\alpha\mathbf{s}\beta), \\ {}^{\mathcal{W}}\mathbf{R}_{\mathcal{B}}(1.2) &= \mathbf{c}\beta\mathbf{s}\alpha(\mathbf{s}\delta\mathbf{s}\eta + \mathbf{c}\delta\mathbf{c}\eta\mathbf{s}\epsilon) - \mathbf{c}\epsilon\mathbf{c}\eta(\mathbf{c}\alpha\mathbf{s}\gamma) \\ &\quad - \mathbf{c}\gamma\mathbf{s}\alpha\mathbf{s}\beta) - (\mathbf{c}\alpha\mathbf{c}\gamma + \mathbf{s}\alpha\mathbf{s}\beta\mathbf{s}\gamma)(\mathbf{c}\delta\mathbf{s}\eta - \mathbf{c}\eta\mathbf{s}\delta\mathbf{s}\epsilon), \\ {}^{\mathcal{W}}\mathbf{R}_{\mathcal{B}}(1.3) &= \mathbf{s}\epsilon(\mathbf{c}\alpha\mathbf{s}\gamma - \mathbf{c}\gamma\mathbf{s}\alpha\mathbf{s}\beta) + \mathbf{c}\epsilon\mathbf{s}\delta(\mathbf{c}\alpha\mathbf{c}\gamma \\ &\quad + \mathbf{s}\alpha\mathbf{s}\beta\mathbf{s}\gamma) + \mathbf{c}\beta\mathbf{c}\delta\mathbf{c}\epsilon\mathbf{s}\alpha \\ , {}^{\mathcal{W}}\mathbf{R}_{\mathcal{B}}(2.1) &= \mathbf{s}\beta(\mathbf{c}\eta\mathbf{s}\delta - \mathbf{c}\delta\mathbf{s}\epsilon\mathbf{s}\eta) + \mathbf{c}\beta\mathbf{s}\gamma(\mathbf{c}\delta\mathbf{c}\eta + \mathbf{s}\delta\mathbf{s}\epsilon\mathbf{s}\eta) \\ &\quad + \mathbf{c}\beta\mathbf{c}\epsilon\mathbf{c}\gamma\mathbf{s}\eta, \\ {}^{\mathcal{W}}\mathbf{R}_{\mathcal{B}}(2.2) &= \mathbf{c}\beta\mathbf{c}\epsilon\mathbf{c}\eta\mathbf{c}\gamma - \mathbf{c}\beta\mathbf{s}\gamma(\mathbf{c}\delta\mathbf{s}\eta - \mathbf{c}\eta\mathbf{s}\delta\mathbf{s}\epsilon) \\ &\quad - \mathbf{s}\beta(\mathbf{s}\delta\mathbf{s}\eta + \mathbf{c}\delta\mathbf{c}\eta\mathbf{s}\epsilon), \\ {}^{\mathcal{W}}\mathbf{R}_{\mathcal{B}}(2.3) &= \mathbf{c}\beta\mathbf{c}\epsilon\mathbf{s}\delta\mathbf{s}\gamma - \mathbf{c}\beta\mathbf{c}\gamma\mathbf{s}\epsilon - \mathbf{c}\delta\mathbf{c}\epsilon\mathbf{s}\beta \\ {}^{\mathcal{W}}\mathbf{R}_{\mathcal{B}}(3.1) &= \mathbf{c}\epsilon\mathbf{s}\eta(\mathbf{s}\alpha\mathbf{s}\gamma + \mathbf{c}\alpha\mathbf{c}\gamma\mathbf{s}\beta) - \mathbf{c}\alpha\mathbf{c}\beta(\mathbf{c}\eta\mathbf{s}\delta - \mathbf{c}\delta\mathbf{s}\epsilon\mathbf{s}\eta) \\ &\quad - (\mathbf{c}\gamma\mathbf{s}\alpha - \mathbf{c}\alpha\mathbf{s}\beta\mathbf{s}\gamma)(\mathbf{c}\delta\mathbf{c}\eta + \mathbf{s}\delta\mathbf{s}\epsilon\mathbf{s}\eta), \\ {}^{\mathcal{W}}\mathbf{R}_{\mathcal{B}}(3.2) &= (\mathbf{c}\gamma\mathbf{s}\alpha - \mathbf{c}\alpha\mathbf{s}\beta\mathbf{s}\gamma)(\mathbf{c}\delta\mathbf{s}\eta - \mathbf{c}\eta\mathbf{s}\delta\mathbf{s}\epsilon) + \mathbf{c}\alpha\mathbf{c}\beta(\mathbf{s}\delta\mathbf{s}\eta \\ &\quad + \mathbf{c}\delta\mathbf{c}\eta\mathbf{s}\epsilon) + \mathbf{c}\epsilon\mathbf{c}\eta(\mathbf{s}\alpha\mathbf{s}\gamma + \mathbf{c}\alpha\mathbf{c}\gamma\mathbf{s}\beta), \\ {}^{\mathcal{W}}\mathbf{R}_{\mathcal{B}}(3.3) &= \mathbf{c}\alpha\mathbf{c}\beta\mathbf{c}\delta\mathbf{c}\epsilon - \mathbf{c}\epsilon\mathbf{s}\delta(\mathbf{c}\gamma\mathbf{s}\alpha - \mathbf{c}\alpha\mathbf{s}\beta\mathbf{s}\gamma) \\ &\quad - \mathbf{s}\epsilon(\mathbf{s}\alpha\mathbf{s}\gamma + \mathbf{c}\alpha\mathbf{c}\gamma\mathbf{s}\beta), \end{aligned}$$

as components of the rotational matrix ${}^{\mathcal{W}}\mathbf{R}_{\mathcal{B}}$ with (row.column).

Therein, \mathbf{c} stands as the abbreviation for \cos and \mathbf{s} for \sin . The angles α , β , γ and η are all over time, but for simplicity written in short version. Same for the whole rotation matrix ${}^{\mathcal{W}}\mathbf{R}_{\mathcal{B}}$.

APPENDIX C

ALIGNMENT MEASUREMENTS

The alignment the patient came with was taken as the initial position. Changes in the I/O-RA alignment were measured

with a disk that was fixed to the knee. An indicator was fixed to the socket. Therefore, when the knee was rotated, the indicator traced the change in degrees. The disk with the indicator can be seen in Figure 14.

Figure 14 shows the CPO in the middle of the VR/VL-A



Fig. 14: CPO adjusting the VR/VL-A by turning the screw on the right side of the adapter. Further, to be seen, the plate and indicator above the knee joint to trace the changes in the I/O-RA alignment.

adjustment. The VR/VL-A was measured in inwards/outwards turns of the screws on the left and right side of the pyramid adapter. Therefore, the CPO paid attention to only do half a turn each time the VR/VL-A was adjusted. The used adapter has the screw grasping at a distance of about 27.5 mm from the rotation center. The screw, being an M8, turns around 1.5 mm per turn which leads to a varus adjustment of about

$$\sin^{-1}\left(\frac{1.5\text{mm}}{27.5\text{mm}}\right) = 3.13\text{degrees}.$$

APPENDIX D

WALKING DIRECTION ESTIMATION

There are several goals of a principal component analysis (PCA) [19]. First, important information can be extracted from a data table. Second, this can be used to compress the size of the data by only keeping the important information. Third, this leads to a simplification in the description of the data set. This sets the grounds for fourth, analysing the structure of the given data. The basis for a PCA is a data matrix or table, denoted by X , build up by objects in n rows and variables in k columns. In our case, it is a two-component model, a projection of a point swarm onto the horizontal plane [20]. The n rows show the observation points in the two columns k which stand for the two axis that are considered.

The data is first centred and then uses the singular value decomposition (SVD) algorithm. The SVD is a generalised version of the eigen-decomposition which forms three simple matrices [19]. Those three matrices are two orthogonal and one diagonal, leading to the left singular vectors, the right singular vectors and the singular values of the data matrix.

With these, the explained variance of the data points can be calculated.

The result of a PCA is a coefficient matrix with the dimension of $k \times k$ [21]. The first row contains the coefficients of the corresponding variables with the biggest variance in the data points. This gives us the components of the vector of the walking direction. The second row contains the coefficients of the variables perpendicular to the first.

APPENDIX E SENSOR-BODY ORIENTATION

To find the relation between shank-sensor frame $\mathcal{S}_{\text{shank}}$ and body of the shank frame \mathcal{B} , the calibration positions, pictured in Figure 8 were used. At rest, the only acceleration measured in each sensor frame \mathcal{S} is the negative acceleration countering the G-force. In the standing position, the measured vector ${}^{\mathcal{S}}e_{\text{stand}}$ is pointing vertically up in space, aligned with the ${}^{\mathcal{W}}z$ vector. In the sitting position, with the feet pointing up, the pointing up vector ${}^{\mathcal{S}}e_{\text{sit}}$ is aligned with the frontal plane of the shank. The norm of ${}^{\mathcal{S}}e_{\text{stand}}$ serves as the unity vector for the y^{VI} axis of frame \mathcal{B}

$${}^{\mathcal{S}}\hat{e}_{\mathcal{B}_y} = \frac{{}^{\mathcal{S}}e_{\text{stand}}}{|{}^{\mathcal{S}}e_{\text{stand}}|}.$$

With a cross product of the y vector and the normed sitting calibration vector ${}^{\mathcal{S}}e_{\text{sit}}$ leads to a unity vector pointing sideways, perpendicular to the PoWD. This vector

$${}^{\mathcal{S}_{\text{shank}}}\hat{e}_{\mathcal{B}_z} = -\hat{e}_{\mathcal{B}_y} \times \frac{{}^{\mathcal{S}}e_{\text{sit}}}{|{}^{\mathcal{S}}e_{\text{sit}}|}$$

serves as the z^{VI} axis of frame \mathcal{B} .

Last, a cross product of the defined y^{VI} and z^{VI} axis leads to the x^{VI} axis, lying horizontally in the PoWD with

$${}^{\mathcal{S}_{\text{shank}}}\hat{e}_{\mathcal{B}_x} = \hat{e}_{\mathcal{B}_z} \times \hat{e}_y.$$

Those three vectors give the alignment of body frame \mathcal{B} in sensor frame $\mathcal{S}_{\text{shank}}$ and are therefore combined to rotation matrix ${}^{\mathcal{S}_{\text{shank}}}\mathbf{R}_{\mathcal{B}}$ with

$${}^{\mathcal{S}_{\text{shank}}}\mathbf{R}_{\mathcal{B}} = [{}^{\mathcal{S}_{\text{shank}}}e_{\mathcal{B}_x} \quad {}^{\mathcal{S}_{\text{shank}}}e_{\mathcal{B}_y} \quad {}^{\mathcal{S}_{\text{shank}}}e_{\mathcal{B}_z}].$$

Now, the final rotational matrix ${}^{\mathcal{W}}\mathbf{R}_{\mathcal{B}}$ can be formed to track the movement of the shank in the FoWD \mathcal{W} with

$${}^{\mathcal{W}}\mathbf{R}_{\mathcal{B}} = {}^{\mathcal{W}}\mathbf{R}_{\mathcal{S}_{\text{shank}}} \cdot {}^{\mathcal{S}_{\text{shank}}}\mathbf{R}_{\mathcal{B}}.$$

The process has to be repeated for the sensor-body orientation between the thigh-sensor frame $\mathcal{S}_{\text{thigh}}$ and the body of the thigh frame \mathcal{T} .

APPENDIX F SWING PHASE

The sensor data was collected over a distance of walking straight for about 12 m. As only the swing phase is regarded, the respective parts had to be extracted from the set. The search for the start and end of the swing was based on the research of [24] which focuses on the angular velocity of the movement of the knee flexion. The beginning of the swing-phase is at the physical toe lift. This is represented by a negative peak in the angular velocity around 10% before the crossing point into the positive. The swing is ended by the termination of forward swing. It is defined with the shank ending its forward angular direction and beginning backward angular motion. This is represented by the angular velocity crossing from positive into negative. It is close to the physical heel strike.

Therefore, code was written in MATLAB regarding the angular velocity of the shank around the Y axis, which represents the knee flexion movement. To start, all negative peaks $peak_{\min}$ were filtered with a minimum peak height that varied with each data set. To smooth out the noise from the beginning for the further calculations, everything before the first minima was set to zero. Onward, all zero-crossings from positive into negative were sought out as $cross_{\text{pos-neg}}$. One swing phase (i) was then defined as

$$peak_{\min}(i) : cross_{\text{pos-neg}}(i).$$

Each swing phase stands for a new step of the regarded leg-side. To avoid acceleration and breaking movements, only the three middle steps were regarded for this research.

APPENDIX G SENSITIVITY ANALYSIS: HIP MOVEMENT

As we hoped to make the estimation of the alignment angles with only one sensor on the shank, the hip movement was first implemented from external sources [25], [26]. However, we also knew that amputees adapt to changes in the alignment of their prosthetic knee and change their movement pattern of the hip accordingly [2], [8]. Therefore, early on, a sensitivity analysis on the hip movement input of the first participant was done.

A bias of +5, +1, -1 and -5 degrees was put on the movement input angles $\alpha(t)$, $\beta(t)$ and $\gamma(t)$ one-by-one, resulting in disturbed input angles $\tilde{\alpha}(t)$, $\tilde{\beta}(t)$ and $\tilde{\gamma}(t)$. The bias was implemented as an offset on the time-dependant movement. This changes the input in Step 1, the calculation of the forward kinematic model, as illustrated in Figure 3. The rotational matrices in Step 1a are therefore calculated with the input of

$$\begin{aligned} &(\tilde{\alpha}(t), \beta(t), \gamma(t), \eta(t), \delta, \epsilon), \\ &(\alpha(t), \tilde{\beta}(t), \gamma(t), \eta(t), \delta, \epsilon) \text{ or} \\ &(\alpha(t), \beta(t), \tilde{\gamma}(t), \eta(t), \delta, \epsilon), \end{aligned}$$

which leads to the calculation of $\tilde{\sigma}(t)$ and $\tilde{\tau}(t)$ as

$$\begin{aligned}\tilde{\sigma}_\alpha/\tilde{\tau}_\alpha & (\tilde{\alpha}(t), \beta(t), \gamma(t), \eta(t), \delta, \epsilon), \\ \tilde{\sigma}_\beta/\tilde{\tau}_\beta & (\alpha(t), \tilde{\beta}(t), \gamma(t), \eta(t), \delta, \epsilon) \text{ or} \\ \tilde{\sigma}_\gamma/\tilde{\tau}_\gamma & (\alpha(t), \beta(t), \tilde{\gamma}(t), \eta(t), \delta, \epsilon).\end{aligned}$$

The inverse fitting for $\tilde{\delta}$ and $\tilde{\epsilon}$ is then calculated with

$$\begin{aligned}\tilde{J} &= \frac{1}{N} \sum_{n=1}^N \|\mathcal{W}_{\tilde{\sigma}_{\text{FKM}}}(t) - \mathcal{W}_{\sigma_{\text{meas}}}(t)\|^2 + \|\mathcal{W}_{\tilde{\tau}_{\text{FKM}}}(t) - \mathcal{W}_{\tau_{\text{meas}}}(t)\|^2, \\ \min \frac{1}{T} \sum_{t=1}^T \tilde{J} & \text{ over } \tilde{\delta}, \tilde{\epsilon} [-10^\circ, 10^\circ].\end{aligned}$$

We wanted to see how much each movement (rotation, abduction, flexion) of the hip would change the end-results of Step 2a to the disturbed results $\tilde{\delta}$ and $\tilde{\epsilon}$. The sensitivity analysis was done on the walking trial with the optimal alignment. The optimal alignment was chosen by the CPO, in agreement with the participant.

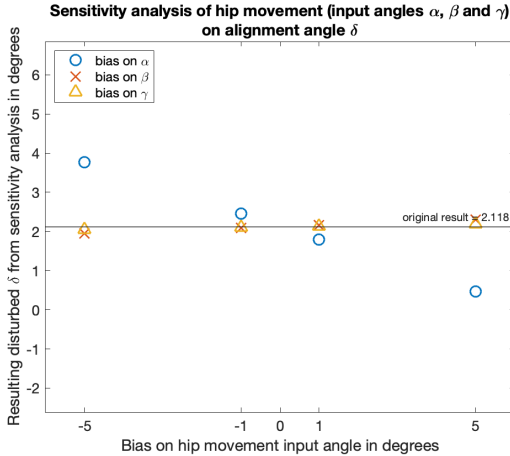


Fig. 15: Sensitivity analysis on hip movement input - resulting disturbed $\tilde{\delta}$

Figure 15 shows the impact of a bias on the three different movement inputs on $\tilde{\delta}$. As δ is the rotational adjustment angle, the sensitivity analysis shows what we assumed. A bias on the rotational input $\alpha(t)$ shows the biggest influence. However, the slope of the linear trend is not 1. The assumption was, that a rotation of the hip leads to a rotation of the shank with the same amount, as the prosthetic knee only has one degree of freedom. The fact that the slope is smaller could be due to the fact, that in step 2, the inverse kinematic mapping, the fitting happens for both adjustment angles δ and ϵ at the same time. Disturbances in the abduction and flexion movement input of the hip show very small effect on the result.

Figure 16 shows the impact of a bias on the three different movement inputs on $\tilde{\epsilon}$. We expected the abduction movement

to have a biggest influence on the varus/valgus adjustment angle. This assumption was confirmed. However, again the slope is smaller than expected. The other movements again show small effect on the result.

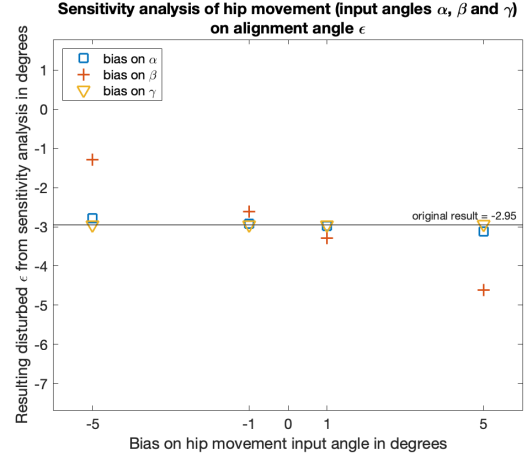


Fig. 16: Sensitivity analysis on hip movement input - resulting disturbed $\tilde{\epsilon}$

Table III shows the calculated results for $\tilde{\delta}$ and $\tilde{\epsilon}$ with changed bias on the hip movement input one-by-one.

bias on $\alpha(t)$	$\tilde{\delta}_\alpha$	$\tilde{\epsilon}_\alpha$
+5	0.46132	-3.1191
+1	1.7868	-2.9847
0	2.118	-2.9504
-1	2.4492	-2.9159
-5	3.7735	-2.7753

bias on $\beta(t)$	$\tilde{\delta}_\beta$	$\tilde{\epsilon}_\beta$
+5	2.304	-4.6171
+1	2.1538	-3.2838
0	2.118	-2.9504
-1	2.0828	-2.617
-5	1.9481	-1.2836

bias on $\gamma(t)$	$\tilde{\delta}_\gamma$	$\tilde{\epsilon}_\gamma$
+5	2.1906	-2.9399
+1	2.1326	-2.9488
0	2.118	-2.9504
-1	2.1034	-2.9517
-5	2.0448	-2.9545

TABLE III: Sensitivity analysis on hip movement Bias on $\alpha(t)$, $\beta(t)$ and $\gamma(t)$ input angles of hip movement

APPENDIX H

SENSITIVITY ANALYSIS: SENSOR-BODY ORIENTATION

A sensitivity analysis is performed on the rotation matrix between the shank and the shank-sensor ${}^{\mathcal{S}_{\text{shank}}}\mathbf{R}_\beta$. The sensitivity analyses on the sensor-body orientation was also done for the walking trial with the optimal alignment. To analyse the effect of a disturbance on the orientation, an additional disturbed frame, $\tilde{\mathcal{B}}$, is introduced. This biased body frame is

bias around x	$\hat{\delta}_x$	$\hat{\epsilon}_x$
+5	-0.67675	-4.9168
+1	0.052282	-3.1893
0	0.25118	-2.7402
-1	0.45537	-2.2856
-5	1.3079	-0.42762

bias around y	$\hat{\delta}_y$	$\hat{\epsilon}_y$
+5	-0.14905	-3.2685
+1	0.17907	-2.8421
0	0.25118	-2.7402
-1	0.31974	-2.64
-5	0.5619	-2.2522

bias around z	$\hat{\delta}_z$	$\hat{\epsilon}_z$
+5	-0.56927	-1.4741
+1	0.048678	-2.5066
0	0.25118	-2.7402
-1	0.45276	-2.9737
-5	1.2477	-3.9042

TABLE IV: Bias on sensor-body orientation Rotations around x , y , and z axis of body frame \mathcal{B}

rotated individually around ${}^B x$, ${}^B y$ and ${}^B z$ by ± 5 degrees with respect to body frame \mathcal{B} . The disturbed rotation matrix between sensor frame \mathcal{S} and disturbed frame $\hat{\mathcal{B}}$ was calculated as

$${}^S \mathbf{R}_{\hat{\mathcal{B}}} = {}^S \mathbf{R}_{\mathcal{B}} \cdot {}^B \mathbf{R}_{\hat{\mathcal{B}}},$$

with the rotation matrix between body frame \mathcal{B} and $\hat{\mathcal{B}}$ depending on the chosen axis rotation

$$\begin{aligned}
 {}^B \mathbf{R}_{\hat{\mathcal{B}},x} &= \begin{bmatrix} 1 & 0 & 0 \\ 0 & \cos(\phi_r) & -\sin(\phi_r) \\ 0 & \sin(\phi_r) & \cos(\phi_r) \end{bmatrix}, \\
 {}^B \mathbf{R}_{\hat{\mathcal{B}},y} &= \begin{bmatrix} \cos(\chi_r) & 0 & \sin(\chi_r) \\ 0 & 1 & 0 \\ -\sin(\chi_r) & 0 & \cos(\chi_r) \end{bmatrix} \text{ or} \\
 {}^B \mathbf{R}_{\hat{\mathcal{B}},z} &= \begin{bmatrix} \cos(\psi_r) & -\sin(\psi_r) & 0 \\ \sin(\psi_r) & \cos(\psi_r) & 0 \\ 0 & 0 & 1 \end{bmatrix}.
 \end{aligned}$$

If the rotation disturbance around the x axis is regarded, ϕ_r is set to a value of -5 , -1 , 1 or 5 degrees. For the rotation disturbance around the y axis, the value for χ_r is adapted and for the z axis, the value for ψ_r . The artificial disturbances take effect on Step 1a of the calculation towards an algorithm, illustrated in Figure 3. This modifies the result of Step 1c to disturbed deviations of $\hat{\sigma}_{FKM}(t)$ and $\hat{\tau}_{FKM}(t)$ and the proximate result of Step 2a) to disturbed estimated adjustment angles $\hat{\delta}$ and $\hat{\epsilon}$ with

$$\begin{aligned}
 \hat{J} &= \frac{1}{N} \sum_{n=1}^N \|\mathcal{W}_{\hat{\sigma}_{FKM}}(t) - \mathcal{W}_{\sigma_{meas}}(t)\|^2 + \|\mathcal{W}_{\hat{\tau}_{FKM}}(t) - \mathcal{W}_{\tau_{meas}}(t)\|^2, \\
 &\min \frac{1}{T} \sum_{t=1}^T \hat{J} \text{ over } \hat{\delta}, \hat{\epsilon} [-10^\circ, 10^\circ].
 \end{aligned}$$

Table IV shows the calculated results for $\hat{\delta}$ and $\hat{\epsilon}$ with changed bias on the hip movement input one-by-one. With these disturbed end results, the sensitivity of the sensor-body calibration Sensitivity_{SB} is calculated one-by-one for each axis rotation value and separately for δ and ϵ according to the following formulas

$$\begin{aligned}
 \text{Sensitivity}_{SB,\delta} &= \delta_{est} - \hat{\delta}, \\
 \text{Sensitivity}_{SB,\epsilon} &= \epsilon_{est} - \hat{\epsilon}.
 \end{aligned}$$

δ_{est} and ϵ_{est} are the undisturbed estimated adjustment angles obtained with the measurement input (Step 2a), explained in chapter III.

The results for the sensitivity analysis of the sensor-body orientation are shown in section VIII-C and discussed in section IX-C.

APPENDIX I
RESULTS

This section shows all the calculated results for both experiments, split in several tables. Table V shows the allocation of the individual sensors to their position. This is needed to differentiate between the data packages, provided by the software from Xsens.

	Hip	Thigh	Shank
Left	00B44058	00B44112	00B44113
Right	00B44109	00B43F80	00B43F80

TABLE V

Every trial is assigned three measurements. The standing calibration, the sitting calibration and the walking trial. Trial 006 is the only trial with four measurements. This was the first time the rotation adjustment angle δ was adjusted. Measurement 017 was done without rotating the foot in the opposite direction as the shank. This was found out to be necessary though, to guarantee a good basis for the participant to walk.

Table IX shows the results for the calculated estimation of δ and ϵ for the second participant.

Attention! in the second experiment, from trial 009 onwards, the sitting and standing calibration position was switched around. This was done for the comfort for the patient.

TABLE VI: Results for first participant, part I

Trial	Nr. Meas	Task	Set δ	$\hat{\delta}_{opt}$	$\hat{\delta}_{prop}$	$\hat{\delta}_{est}$	Set ϵ	ϵ_{opt}	ϵ_{prop}	ϵ_{est}	Comments by participant
001	m 000	standing									
	m 001	sitting									
	m 002	walking	0	-1.3461	-0.3836	-0.9625	0	1.3096	-1.8124	3.122	Initial basis
002	m 003	standing									
	m 004	sitting									
	m 005	walking	0	-1.1367	0.1833	-1.320	-1/2	0.21583	0.74253	-0.5267	feeling of falling outwards
003	m 006	standing									
	m 007	sitting									
	m 008	walking	0	1.8204	0.0614	1.759	-1	0.62879	-1.47021	2.099	little difference to previous
004	m 009	standing									
	m 010	sitting									
	m 011	walking	0	-3.0059	-3.2295	0.2236	1/2	0.29066	2.829	-2.5384	he can life with that nicely
005	m 012	standing									
	m 013	sitting									
	m 014	walking	0	-2.3443	-3.4193	1.075	+1	0.49671	3.435	-2.938	more pressure on stump, outside further downwards, inside further upwards
006	m 015	standing									
	m 016	sitting									
	m 017	walking									falling diagonally to the front, foot feels lurching and vibrating
007	m 018	walking									
		foot rotated	-5	4.0217	-2.6453	6.667	+1	-1.4227	5.119	-6.542	way better with the additional foot rotation
	m 019	standing									
008	m 020	sitting									
	m 021	walking	-5	-1.6618	-3.4738	1.812	+1/2	2.8006	3.046	0.3977	the forward sway feels quite tiresome
	m 022	standing									
	m 023	sitting				ss_00					
	m 024	walking	-5	6.6666	-0.001	6.667	0	-4.4816	1.190	-5.6711	easier than previous but still feeling like there is a resistance while swaying forwards

TABLE VII: Results for first participant, part II

Trial	Nr. Meas	Task	Set δ	δ_{opt}	δ_{prop}	δ_{est}	Set ϵ	ϵ_{opt}	ϵ_{prop}	ϵ_{est}	Comments by participant
009	m 025	standing									
	m 026	sitting									
	m 027	walking	-5	5.5582	-1.1088	6.667	-1/2	-2.0782	1.520	-3.598	resistance feels higher and additional feeling like falling outwards
010	m 028	standing	-5	4.4866	-1.5365	6.0231	-1	0.17596	0.967	-0.79096	
	m 029	sitting									
	m 030	walking									falling outwards, resistance less than previous
011	m 031	standing									
	m 032	sitting									
	m 033	walking	+5	-0.528	1.4526	-1.9806	-1	1.5449	0.554	0.9912	falling outwards, feeling pressure in the back of the stump while bending the knee
012	m 034	standing									
	m 035	sitting									
	m 036	walking	+5	-0.3718	0.6186	-0.9904	-1/2	1.1633	-0.762	1.9254	falling outwards, foot turns outwards, pressure in the socket on the whole inside
013	m 037	standing									
	m 038	sitting									
	m 039	walking	+5	-1.3259	-0.2794	-1.0465	0	1.1125	-0.006	1.1188	quite nice, very easy to bend knee in the first instance
014	m 040	standing									
	m 041	sitting									
	m 042	walking	+5	-2.4469	-0.3733	-2.0736	+1/2	0.87449	-0.641	1.515	feeling his whole stump
015	m 043	standing									
	m 044	sitting									
	m 045	walking	+5	-3.0829	-1.2737	-1.8092	+1	0.33426	1.420	-1.0862	not bad but foot a bit turbulent
016	m 046	standing									
	m 047	sitting									
	m 048	walking	+5	-2.9787	0.3219	-3.3006	+1 1/2	-0.12713	1.056	-1.1829	needs force from thigh to bring prosthesis to the front

TABLE VIII: Results for first participant, part III

Trial	Nr. Meas	Task	Set δ	δ_{opt}	δ_{prop}	δ_{est}	Set ϵ	ϵ_{opt}	ϵ_{prop}	ϵ_{est}	Comments by participant
017	m 049	standing									
	m 050	sitting									
	m 051	walking	0	-1.5244	-1.05531	-0.46909	+1 1/2	-1.3753	4.001	-5.3767	pressure on frontal part of stump
018	m 052	standing									
	m 053	sitting									
	m 054	walking	-5	0.50197	-2.13213	2.6341	+1 1/2	-0.39174	3.161	-3.5528	swaying a bit
019	m 055	standing									
	m 056	sitting									
	m 057	walking	+10	0.44625	1.17053	-0.72428	+1 1/2	0.5258	0.5502	0.20095	swaying a lot, having problems with whole step
020	m 058	standing									
	m 059	sitting									
	m 060	walking	+10	-1.3807	-1.55562	0.17502	+1	0.43342	-0.218	0.65179	feeling of falling outwards
021	m 061	standing									
	m 062	sitting									
	m 063	walking	+10	-2.0947	-1.23474	-0.85996	+1/2	0.34577	0.115	0.23112	falling even more, also towards the front, additionally touching other leg
022	m 064	standing									
	m 065	sitting									
	m 066	walking	+5	1.3635	-1.5849	2.9484	+1/2	-1.4985	3.100	-4.5989	was good already, done again
023	m 067	standing									
	m 068	sitting									
	m 069	walking	+3	-1.0928	-1.344	0.2512	+1/2	-0.49204		-2.7402	optimal settings

TABLE IX: Results for second participant

	Measurement	Task	Set δ	δ_{est}	Set ϵ	ϵ_{est}	Comments by participant
Trial 001	m 000	standing					
	m 001	sitting					
	m 002	walking	0	5.069	0	-0.79634	initial basis
Trial 002	m 003	standing					
	m 004	sitting					
	m 005	walking	0	-4.3858	+1	2.3305	falling outwards
Trial 003	m 006	standing					
	m 007	sitting					
	m 008	walking	0	-2.7176	+1/2	2.9993	not standing right under the socket
Trial 004	m 009	standing					
	m 010	sitting					
	m 011	walking	0	6.6665	-1/2	-3.6856	falling inwards
Trial 005	m 012	standing					
	m 013	sitting					
	m 014	walking	0	6.6666	-1	-4.4447	even more than previous
Trial 006	m 015	standing					
	m 016	sitting					
	m 017	walking	-5	6.6667	-1	-4.5294	knee is not going straight, swaying
Trial 007	m 018	standing					
	m 019	sitting					
	m 020	walking	-5	-6.7571	-1/2	-7.7494	a bit more stable than previous, but still swaying
Trial 008	m 021	standing					
	m 022	sitting					
	m 023	walking	-5	-7.0332	0	2.8952	socket straight but no straight movement of foot
Trial 009	m 024	sitting					
	m 025	standing					
	m 026	walking	-5	-4.2601	+1/2	3.7129	almost no difference to previous
Trial 010	m 027	sitting					
	m 028	standing					
	m 029	walking	-5	6.6666	+1	-2.7082	swaying foot more extreme, body falling outwards
Trial 011	m 030	sitting					
	m 031	standing					
	m 032	walking	+5	2.0637	+1	-0.2014	swaying of leg backwards, falling outwards
Trial 012	m 033	sitting					
	m 034	standing					
	m 035	walking	+5	4.2493	+1/2	-2.3172	less extreme than previous, less swaying
Trial 013	m 036	sitting					
	m 037	standing					
	m 038	walking	+5	-1.2132	0	-2.537	almost no difference to previous
Trial 014	m 039	sitting					
	m 040	standing					
	m 041	walking	+5	5.863	-1/2	-5.5029	being pushed inwards, really not comfortable
Trial 015	m 042	sitting					
	m 043	standing					
	m 044	walking	+5	-12.8558	-1	-4.0747	even worse than previous
Trial 016	m 045	sitting					
	m 046	standing					
	m 047	walking	0	1.3608	0	-2.0055	best option

APPENDIX J INFORMATION SHEET AND CONSENT FORM

Information sheet for “Creating an algorithm to optimise gait pattern for patients with above knee prosthesis with the use of sensors from Xsens”

Purpose of the research

From literature, it is well defined how a safe and stable alignment for leg prosthesis can be achieved by alignment in the sagittal plane. However, there is little information available on the alignment in the transversal and frontal plane. This study concentrates on small changes in the frontal and transversal plane to get a smooth and comfortable swing phase movement. With an optimised gait pattern, discomforts in the back as well as flaws in the posture can be reduced, which leads to an overall increase of the quality of life of the amputee.

For the research, up to six wireless motion track sensors, “MTw Awinda” from Xsens, are attached with straps to the lower body (hip, socket and shank-tube of the prosthesis and potentially the other leg) of the participant which is in the aligning process. The participant walks as part of the alignment process instructed by the CPO.

The participation will be part of a Master thesis with the goal to find an algorithm that can predict how the alignment of a prosthesis can be adapted to result in a smooth gait.

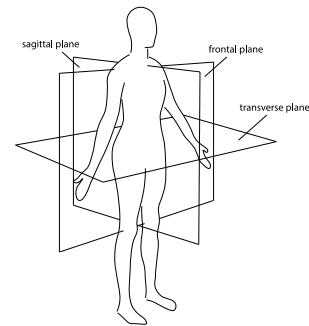


Figure 1: Planes with respect to the body

Benefits and risks of participating

No risk is expected from the attaching of the sensors to the body of the participant. The use of velcro or elastic strips will ensure the attachment to be comfortable and not restrictive for the participant. No additional risk, due to the attached sensors, is expected from the usual alignment process.

Withdrawal from the study

The participant can withdraw from the study at any point. If the participant wants to withdraw from the study, all they have to do is tell the researchers that they want to stop participation. The researchers will be present at all times.

In consideration between the researchers and the participant, the potential recorded data until this point can be used for research or will be deleted immediately.

The further alignment process by the CPO will not be affected.

Collection and retention of personal information

Personal information like age, body length, side of amputation, height of amputation and satisfaction of gait will be collected. All the data will be saved anonymously. Together with the measured sensor data it will be used for the Master Thesis of Christine Amelie Palm.

At any point, the participant can request to access the data, change it or have it erased.

Consent Form for
“Creating an algorithm to optimise gait pattern for patients with
above knee prosthesis with the use of sensors from Xsens”

Please tick the appropriate boxes

	Yes	No
Taking part in the study		
I have read and understood the study information dated 14/10/2019, or it has been read to me. I have been able to ask questions about the study and my questions have been answered to my satisfaction.	<input type="checkbox"/>	<input type="checkbox"/>
I consent voluntarily to be a participant in this study and understand that I can refuse to answer questions and I can withdraw from the study at any time, without having to give a reason.	<input type="checkbox"/>	<input type="checkbox"/>
I understand that taking part in the study involves pictures being taken from my prosthetic build-up and the different alignments being written down. Sensors will be attached, with the help of straps, to my lower body and my prosthesis. The sensors are wireless inertial-magnetic motion trackers. They will record angular velocity, acceleration and magnetic field change due to my movements while I am in the alignment process with the prosthetist. The data is saved for further analysis within the scope of this research.	<input type="checkbox"/>	<input type="checkbox"/>
Apart from the sensor measurement I understand that I will be asked questions concerning generic information like age, height and side of amputation. Further questions about the level of comfort while walking will be asked. This information is going to be written down and also going to be saved for further analysis within the scope of this research.	<input type="checkbox"/>	<input type="checkbox"/>
Use of the information in the study		
I understand that information I provide will be used for the Master Thesis written by Christine Amelie Palm	<input type="checkbox"/>	<input type="checkbox"/>
I understand that personal information collected about me that can identify me, such as my name or where I live, will not be shared beyond the study team	<input type="checkbox"/>	<input type="checkbox"/>
I agree that my information can be quoted (anonymous) in research outputs	<input type="checkbox"/>	<input type="checkbox"/>
I agree that photos of my prosthetic alignment (anonymous) can be published	<input type="checkbox"/>	<input type="checkbox"/>
Future use and reuse of the information by others		
I give permission for the anonymised data from the gait analysis in combination with information about the prosthesis and the satisfaction outcome that I provide to be archived by Christine Amelie Palm so it can be used for future research and learning.	<input type="checkbox"/>	<input type="checkbox"/>

Signatures

Name of participant

Signature

Date

I have accurately read out the information sheet to the potential participant and, to the best of my ability, ensured that the participant understands to what they are freely consenting.

Researcher name

Signature

Date

Study contact details for further information:

Christine Amelie Palm
c.palm@hotmail.com
+31613949282

